分类号 …….. 密级……
ＵＤＣ …… 编号……

中 南 大 学

CENTRAL SOUTH UNIVERSITY

硕士学位论文

论 文 题 目　Cu-Sn-Ti 体系扩散偶界面反应的研究
学科、专业　材 料 学
研究生姓名　李 大 建
导师姓名及
专业技术职称　金 展 鹏 教 授

CENTRAL SOUTH UNIVERSITY

MASTER'S DEGREE THESIS

The study on Interfacial Reactions of Cu-Sn-Ti System with Diffusion Couple Technical

Graduate: **Li Dajian**

Department: Materials Science and Engineering

Supervisor: **Jin Zhanpeng (Prof.)**

Abstract

The Cu-Sn-Ti ternary system and its three boundary binary systems are of critical importance in practice. The Ti/Sn and Cu/Sn solid/liquid diffusion couples and the Cu/Ti diffusion couples are made and examined. Only Sn_3Ti_2 forms if Ti/Sn solid/liquid diffusion couples are annealed at 873K for 30~160 minutes. When annealed at 808K for 10 minutes, only Cu_3Sn forms in Cu/Sn solid/liquid diffusion couple. With the annealed time increasing, $Cu_{41}Sn_{11}$ layer forms between Cu and Cu_3Sn in 30 mins, and then Bcc_a_2 layer forms between Cu and $Cu_{41}Sn_{11}$ in 60 mins. After annealing at 1023K for 1000 hours, four compounds, $CuTi_2$, CuTi, Cu_4Ti_3 and Cu_4Ti form in Cu/Ti diffusion couple while Cu_3Ti_2 is absent. The interfacial reaction process and phase formation sequence has been predicted with the maximum driving force model using the Thermo-Calc software.

Phase relations in the Sn-Cu side of the Cu-Sn-Ti system at 823K were determined by diffusion-triple approach along with Electron Probe Microanalysis (EPMA) technique. A ternary phase, CuSnTi, was detected to have a certain homogeneity range. Except in the Ti-rich corner, phase equilibria in most part of the isothermal section of Cu-Sn-Ti ternary system at 823K were well established. In this isothermal section, 12 three-phase equilibria were proposed, of which 2 three-phase equilibria, $CuTi_2$+Sn_5Ti_6+Ti and CuSnTi+Cu_4Ti_3+Cu_4Ti need further study.

The Cu/Ti diffusion couples annealed at 1023K for 1000h was annealed with molten Sn at 823K for 15 to 480 mins. With addition of Ti, the consumption speed of Cu is greatly enhanced. At 823K, Cu plate with thickness of about 3mm solute into Sn in less than 15 mins. Cu-Ti binary

compounds still have different consumption speed in molten Sn. The grown out Cu-Ti binary compounds show great anisotropism in this work, and there are quick diffusion paths vertical to Cu-Ti interface form in them. With progressing of annealing, different tri-junctions which mean correlative three-phase regions in the isothermal section appear in the samples sequently at 823K. After annealed at 823K for different times from 15 to 480 mins, the morphologies of diffusion zones are illustrated with diffusion paths.

KEY WORDS: diffusion, intermetallics, phase diagram, solid-liquid reaction, microstructure

摘要

在材料研究的过程中，相图扮演着极其重要的角色，因为它提供了所研究体系中多种可能的亚稳相变的背景及分配系数。虽然现在已经可以利用计算得到很多复杂的相图，短期内实测相图仍然具有不可被替代的重要性。人们采用了很多方法来实际测量相图，其中最重要，也是最有效的方法之一就是扩散偶法。

扩散偶就是将两块或几块材料（主要是金属）紧密接触在一起，在一定温度下使其相互扩散并发生反应。保温一段时间后淬火急冷，保持其高温下的组织并进行分析的一种实验方法。基于局部平衡的假设，并利用扩散过程中，在一个扩散偶样品中便可覆盖一个二元系或三元系中所有成分的特性，就可以利用一个样品得到一个等温截面。和传统的合金法测相图相比，扩散偶法可以大幅度提高相图研究的效率。

活化焊接（active braze）是目前被广泛采用的连接陶瓷与金属的工艺，在焊料中添加 Ti 等表面活性元素, 可使其润湿性得到明显改善。T i, Zr, Hf, Pd 等过渡族或稀有金属元素具有较强的化学活性, 加至焊料中后在高温下对氧化物、硅酸盐具有亲和性, 可和 Cu, Ni, Ag, A u,等一同制成陶瓷-金属焊接活性焊料。活性焊料在二界面处可以产生机械或化学结合。机械结合可以认为是焊料质粒嵌入或渗入陶瓷表层微孔区, 而化学结合强度归结于焊料和基体间的物质转移和反应。陶瓷界面上的反应会大大促进润湿性。AgCuT i 三元焊料系列, 对大多数工程陶瓷表面有润湿性, 在高温下伴随着液固界面的化学反应和传质扩散, 从而在界面形成固溶体相和新化合物相，可提高表面强度。

虽然 AgCuTi 三元系焊料被广泛采用，但是它们的强度及剪切强度还是比较低，并不适用连接铁基的金刚石工具（主要是刀具）。所以有人加入 Ni、Fe、Cr 等元素来提高焊料合金的强度，但这些元素又会在高温下促使金刚石向石墨转变，反而降低了金刚石的强度。还有人采用增加焊料中沉淀强化相数量，如 Si_3N_4、TiC、SiC、WC 等的办法来改良焊料的性能，取得了一定的效果。但这种做法又带来了新的问题，就是强化相的数量不可以过多，以便在焊接过程中保持足够多的液相剩余，保证焊接质量。

目前为止，Cu-Sn-Ti 焊料是在这个方面 Cu-Ag-Ti 焊料的最佳替代者，可以使金刚石刀具的切削速度及使用寿命均得到提高。这主要是由于 Sn 的存在，造成焊料中 Ti 的活性降低，使活化焊接时表面生成强化相的同时在液相中仍可保持较高的 Ti 浓度，在液相中生成 Ti-Sn 的强化相，提高工具性能。

不仅 Cu-Sn-Ti 三元系具有重要的实际应用价值，而且它的三个边际二元系也都具有广阔的实际应用领域。Cu-Sn 二元系由于其在电子工业的广泛应用已经被多次研究。金属 Ti 由于其具有良好的物理性能和化学性能而作为电子封装中的焊点下金属（UBM）层电镀在待焊接的电子器件上。在高强高导铜合金的制备过程中加入 Ti 可以使其在保持良好的导电性的同时获得较高的强度。

本文首先制备了 Cu-Sn-Ti 三元系相关的边际二元系的扩散偶，其中 Ti-Sn 及 Cu-Sn 两个二元系为固-液扩散偶，Cu-Ti 二元系为固态扩散偶，在不同温度下退火不同的时间，利用扫描电镜和电子探针分析了其扩散层组织。Ti/Sn 固-液扩散偶在 873K 下退火 30~160mins 时，只有 Sn_3Ti_2 相生成。Cu/Sn 固-液扩散偶在 808K 下退火 10mins 时，

只有 Cu_3Sn 相生成。当退火时间延长至 30mins 后在 Cu 与 Cu_3Sn 的界面上生成了 $Cu_{41}Sn_{11}$。退火 60mins 后在 Cu 与 $Cu_{41}Sn_{11}$ 的界面上又生成了 Bcc_a_2。Cu/Ti 二元固相扩散偶在 1023K 下退火 1000h 后，生成了 $CuTi_2$，CuTi，Cu_4Ti_3，Cu_4Ti 4 个化合物，而 Cu_3Ti_2 相并未在扩散偶中出现。

对于 Cu-Sn-Ti 相关二元系的界面反应产物及相的生成序列采用 Thermocalc 软件，依据最大驱动力模型对其相形成序列及形貌进行了预测。预测结果和实验结果吻合得很好。

值得注意的是，在 Lee 等人提出最大驱动力模型的文章中，只提到了最大驱动力模型可以用来预测界面反应中第一个生成的相。而在本文中除 Sn-Ti 二元系只有一个中间化合物生成外，Cu-Sn 二元系在 808K 下依次生成了该温度下所有的三个化合物，而 Cu-Ti 二元系则是在退火 1000 小时后生成了 4 个化合物，只有一个 Cu_3Ti_2 一个化合物没有在扩散偶中出现。本文利用扩散偶试样中，一旦生成了中间化合物，则出现新的亚稳平衡的特点，反复使用最大驱动力模型，成功解释了所出现的实验现象。

将 1023K 下退火 1000 小时得到的 Cu/Ti 二元扩散偶与含 Cu 量为 20wt.%的 Cu-Sn 溶液在 823K 下做成固-固/液三元扩散偶，退火 30~480mins，利用扫描电镜及电子探针分析得到该三元系在 823K 时的相关系。

在对退火不同时间得到的扩散偶样品进行分析时，发现不同退火时间的扩散偶中所出现的相及其相关系都是相同的。只有 Sn_3Ti_2、Cu_3Sn、CuSnTi 和 liquid 相的平衡关系比较模糊，经过对这四个相的

数量、形貌、分布位置及在不同的扩散偶中的相对变化，确定了其相关系为 liquid+Sn_3Ti_2+CuSnTi 和 liquid+CuSnTi+Cu_3Sng 两个三相平衡。

由于 CuSnTi 三元相与 Cu-Sn 化合物接触部分的形貌非常复杂，即使采用电子探针技术也无法确定其精确的截线。本文采用 CuSnTi 三元相为计量比化合物及 Cu-Sn 二元化合物中 Ti 的溶解度可忽略不计的假设，将 CuSnTi 的成分从得到的成分数据中去除，与 Cu-Sn 二元化合物相比较，得到合理的结果，从而大致确定了它们之间的截线。

本工作最终得到的 Cu-Sn-Ti 三元系在 823K 下的等温截面如图 1 所示。

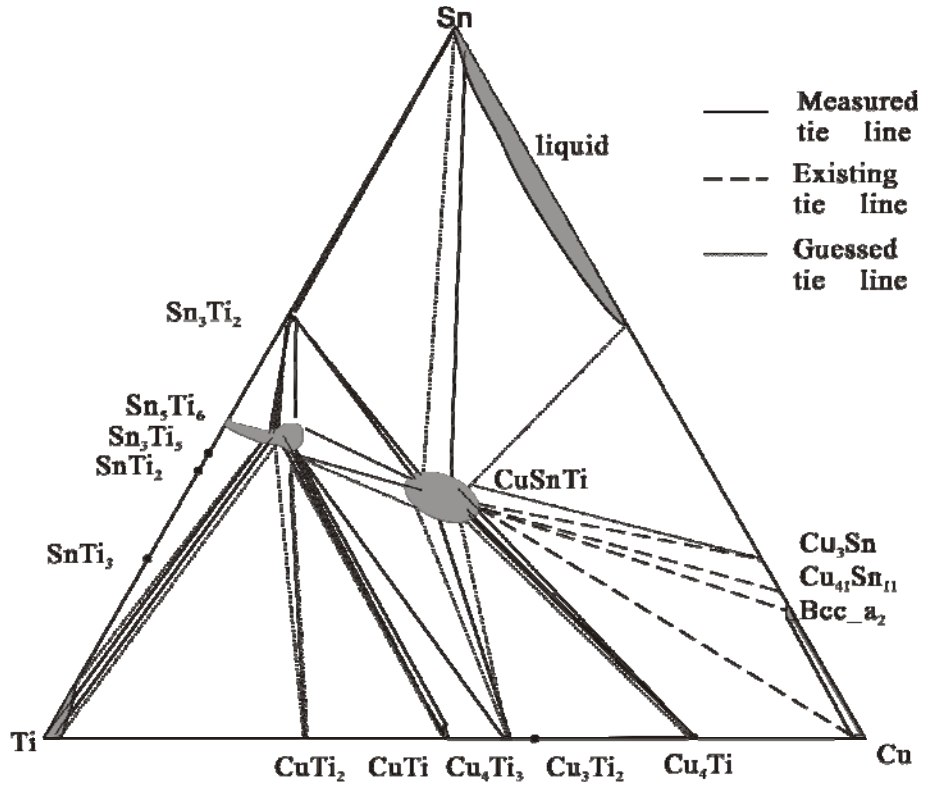

图 1 实验测得的 Cu-Sn-Ti 三元系 823K 下的等温截面（实线表示在局部平衡假设下，采用 EPMA 测量的数据外推得到的截线；虚线表示扩散偶上实际存在的，但是不能精确测量的线；用点表示的虚线是为了满足相律估计的截三角形）。

在本工作中发现 823K 下，只有一个三元中间化合物 CuSnTi 存在，并且存在一定的成分范围。在 Cu-Sn-Ti 三元扩散偶中总共检测到 12 个三相平衡，根据相律，其中 $CuTi_2$+CuTi+Sn_5Ti_6、Sn_5Ti_6+Sn_3Ti_2+CuSnTi、Liquid+Sn_3Ti_2+CuSnTi, Liquid+CuSnTi+Cu_3Sn、CuTi+Cu_4Ti_3+Sn_5Ti_6 、 CuSnTi+Cu_4Ti_3+Sn_5Ti_6 、 CuSnTi+Cu_3Sn+$Cu_{41}Sn_{11}$ 、CuSnTi+$Cu_{41}Sn_{11}$+Bcc_a_2、CuSnTi+Cu_4Ti+Cu、CuSnTi+Bcc_a_2+Cu 等 10 个三相平衡是可以确定的。由于没有在扩散偶试样中发现 Sn_5Ti_6、$SnTi_2$、$SnTi_3$ 和 Cu_3Ti_2 等应稳定存在的边际二元相，造成等温截面富 Ti 角部分仍存在一定的不确定性，而且 $CuTi_2$+Sn_5Ti_6+Ti 和 CuSnTi+Cu_4Ti_3+Cu_4Ti 两个三相平衡也有可能是亚稳平衡，需要进一步研究。

另做了一系列由 Cu/Ti 扩散偶与纯 Sn 反应的固/固/液扩散偶，在 823K 下退火 15~480mins。

从实验结果看出，当有 Ti 参与反应时，Cu 向纯 Sn 中溶解的速度大大提高，所有的 Cu 都在 15 分钟内溶解而消耗掉了。Cu-Ti 的化合物与 Sn 的反应有很明显的方向性。而且随退火时间的延长，Cu-Ti 化合物是由 Cu 一侧到 Ti 一侧依次被消耗掉的。由反应中观测到的液相的快速扩散通道及 Cu-Ti 二元化合物的反应过程可以清楚地发现本实验中生成的 Cu-Ti 二元化合物具有很强的各向异性。

此外，由于反应过程中，Cu-Ti 二元化合物按照一定的方向参与反应，这就使研究从 Cu-Ti 二元化合物到相应的液相的扩散通道成为可能，对退火不同时间的样品进行分析得到相应的扩散通道为：

15 mins：Cu_4Ti_3/CuSnTi//Sn_3Ti_2+liquid/liquid；

30 mins：Cu_4Ti_3/CuSnTi/Sn_3Ti_2/Sn_3Ti_2+liquid/liquid；

120 mins：CuTi/CuTi+Cu_4Ti_3+Sn_5Ti_6/Cu_4Ti_3+Sn_5Ti_6/Cu_4Ti_3+Sn_5Ti_6+CuSnTi/Sn_5Ti_6+CuSnTi/Sn_5Ti_6+CuSnTi+Sn_3Ti_2/Sn_3Ti_2/Sn_3Ti_2+liquid/liquid；

180 mins：$CuTi_2$/$CuTi_2$+CuTi+Sn_5Ti_6/$CuTi_2$+Sn_5Ti_6/Sn_5Ti_6/Sn_5Ti_6+CuSnTi/Sn_5Ti_6+CuSnTi+Sn_3Ti_2/Sn_3Ti_2/Sn_3Ti_2+liquid/liquid；

480 mins：Ti/Ti6Sn5/Ti6Sn5+Sn_3Ti_2/Sn_3Ti_2/Sn_3Ti_2+liquid/liquid。

其相应的扩散通道示意图见图 2：

由图 2(a)~(e)可知随退火时间的延长，扩散通道整体上向 Sn-Ti 一侧移动，这是因为对于 Cu-Ti 扩散偶来说，整体上就是由 Cu 一侧向 Ti 一侧逐渐溶解到液相中去的。

在反应过程中， 先在反应区域内生成 CuSnTi 三元相，随退火时间延长，CuSnTi 三元相又在试样中消失了，取而代之的是 Sn_5Ti_6 相。而在 CuSnTi 消失或 Sn_5Ti_6 相生成时，与它们相邻的 Cu-Ti 二元化合物均为 Cu_4Ti_3。这就意味着 Cu_4Ti_3 既有可能与 CuSnTi 相平衡，又有可能与 Sn_5Ti_6 相平衡。从得到的等温截面上看，这是符合相关系的。结合反应过程中界面的位置，可以看出，当界面位于 Cu_4Ti_3 较靠近 Cu 一侧时，它与 CuSnTi 相平衡，而当位于较靠近 Ti 一侧时则与 CuSnTi 相平衡。这说明虽然 EPMA 结果表明 Cu_4Ti_3 的成分范围很窄，仍然有一个成分梯度存在于得到的 Cu_4Ti_3 层中并可影响到界面反应的产物。

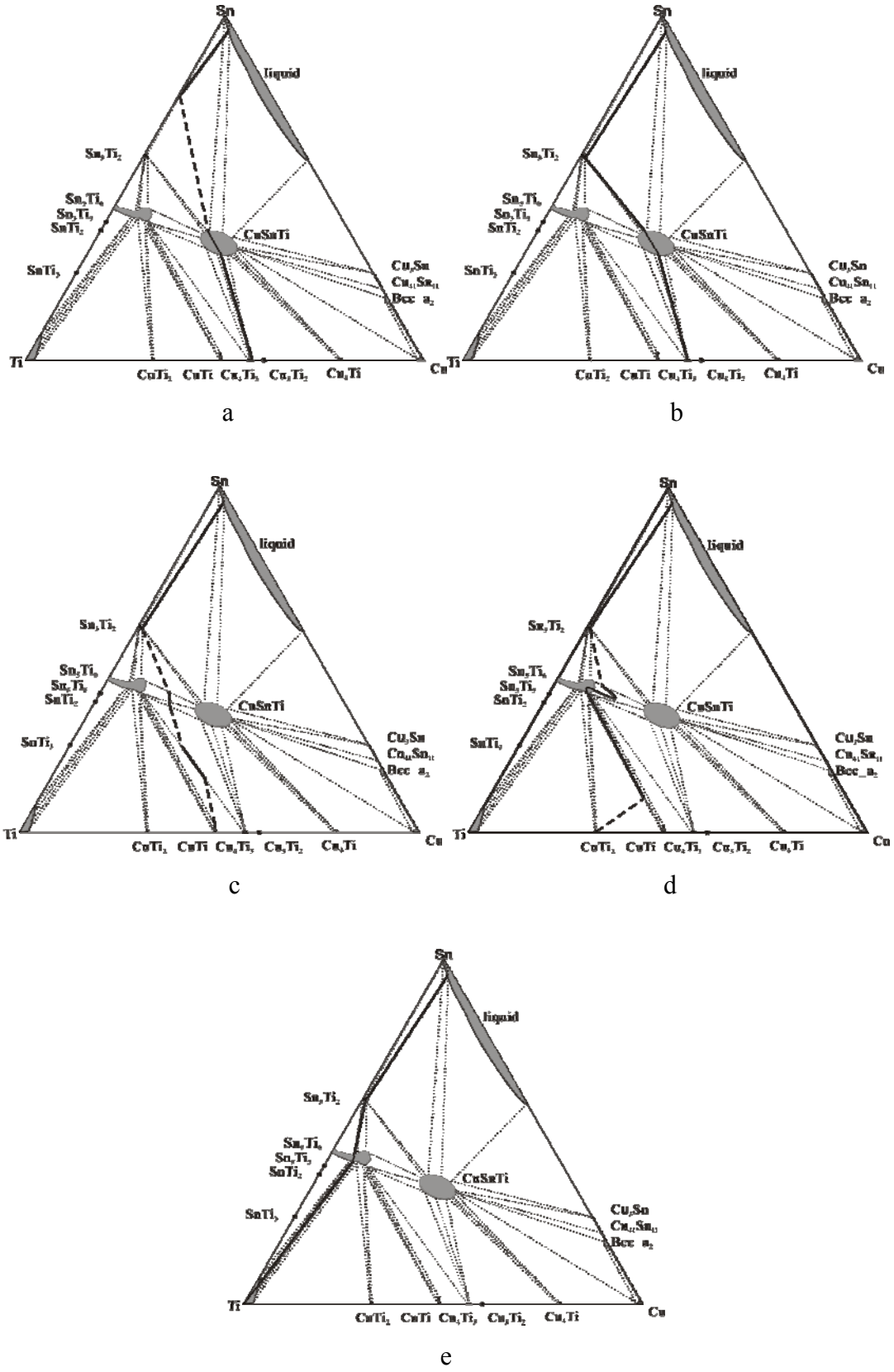

图 2 (Cu/Ti)/Sn 扩散偶在 823 下退火不同时间所对应的扩散通道

(a) 15 mins; (b) 30 mins; (c) 120 mins; (d) 180 mins; (e) 480 mins

在退火时间为 180mins 的样品中，Sn_5Ti_6 相已经取代了绝大多数的 Cu-Ti 二元化合物，但快速扩散通道仍然存在于其中，并且在快速扩散通道周围形成了纺锤状的 CuSnTi 三元相。而在垂直于 Cu/Ti 界面的方向上，Sn_5Ti_6 相和 Sn_3Ti_2 相相邻。这就形成了两个不同的相的空间序列，分别是 Sn_5Ti_6->CuSnTi->liquid 和 Sn_5Ti_6->Sn_3Ti_2->liquid。分析它们的空间位置可以得出由于液相所处的状态不同，基体中的液相可以快速地将溶解的 Cu 与 Ti 扩散出去而降低其浓度；快速扩散通道中的液相则保持了较高的溶质浓度，造成了液相成份的差异，由得到的相图上看来，这种浓度的不同很自然地就会引起了中间化合物类型的差异。

Catalogue

Chapter 1. Preface

1.1. Introduction of diffusion technical

1.1.1. General principles of the diffusion couple method

Phase diagrams play an important role in the understanding of many scientific and technological disciplines, and are important guidelines in the production, processing and application of materials. Though phase equilibria in rather complex systems may be calculated with a certain degree of confidence, the theoretical assessments will likely remain a complementary tool only and not a replacement for experiment. In many experimental methods in phase diagram determination, diffusion couple method is one of the most frequently used techniques [1].

A diffusion couple is simply a pair of metal (or ceramic) blocks of different composition, placed in intimate interfacial contact, and subjected to interdiffusion at a high temperature under the imposed chemical potential gradient. Diffusion couple has long been used to determine phase diagrams and evaluate diffusion coefficients [2]. Based on diffusion couple technical, Diffusion triples (introduced by Hasebe and Nishizawa [3] for simple ternary systems and demonstrated by Jin et al.[4,5] for complex systems with intermetallic compounds) and quadruples [6] have been used to efficiently map ternary and quaternary phase diagrams.

The use of diffusion couples in phase diagram studies is based on the assumption of local equilibria in the diffusion zone. It implies that each infinitely thin layer of such a diffusion zone is in thermodynamic equilibrium with the neighboring layers. In a translated sense, this means that chemical potential (activity) of species varies continuously through the product layers of the reaction zone and has the same value at both sides of an interface.

This concept of local equilibrium being attained at interfaces plays a prominent role in the diffusion theory. It is to be remarked, however, that since diffusion takes place only by virtue of a thermodynamic potential gradient, any system in which

diffusion occurs is not at equilibrium. In other words, for a phase boundary to migrate (i.e. for a reaction product to grow) within the diffusion zone there must be a free energy difference (driving force) which implies some deviation from equilibrium. However, local equilibrium is generally supposed to maintain in the diffusion zone, which means that reaction is very rapid compared with the rate of diffusion.

A diffusion-controlled interaction in a multiphase binary system will invariably result in a diffusion zone with single-phase product layers separated by parallel interfaces in a sequence dictated by the corresponding phase diagram. The reason for the development of only straight interfaces with fixed composition gaps follows directly from the phase rule. Three degrees of freedom are required to fix temperature and pressure and to vary the composition. Reaction morphologies consisting of two-phase structures (i.e. precipitates or wavy interfaces) are, therefore, thermodynamically forbidden, assuming that only volume-diffusion takes place.

In a ternary system, on the other hand, it is possible to develop two-phase areas in the diffusion zone because of the extra degree of freedom. The diffusion zone morphology, which develops during solid-state interaction in a ternary couple, is defined by type, structure, number, shape and topological arrangement of the newly formed phases. The resulting microstructure of the reaction zone can be visualized with the aid of the so-called diffusion path. This is a line on the ternary isotherm, representing the locus of the average composition in planes parallel to the original interface throughout the diffusion zone. Naturally, the diffusion path in a ternary system must fulfil the law of conservation of mass. If no material is lost or created during the interaction, then the diffusion path is forced to cross the straight line between the end-members of the reaction couple (so-called mass balance line) at least once.

Kirkaldy and Brown [7] formulated a number of rules, which relate the composition of the reaction zone to the phase diagram. Later, these rules were conventionalized by Clark [8]. In recent years, the research in multicomponent diffusion took on a new lease of life (Kirkaldy [9], Morral [10] and Ågren [11]), due primarily to the availability of computational power matching the complexity of the available algorithms. Referring for details especially to Ref. 8, it is summarized here the main ideas, using a hypothetical reaction couple of an A–B–C-ternary system shown in Fig. 1.

For a given couple under conditions of chemical equilibrium the reaction path involves a time-independent sequence of intermediate layers. The plot gives information about the order of the product layers, their morphology and their compositions. For example, in the hypothetical system shown in Fig. 1, a solid line crossing a single phase field on the isothermal section (e.g. a–b) denotes an existing layer of that phase in the reaction zone of the couple A/Z. A dashed line parallel to a tie-line in a two-phase field (g–h) represents a straight interface between two single phases. A solid line crossing tie-line on the isotherm (b–c) represents a locally equilibrated two-phase zone (in fact, a wavy interface) in the couple. A solid line entering a two-phase field and returning to the same phase field (d–e–f) represents a region of isolate precipitates. A dashed line crossing a three-phase field (e.g. i–j or k–l) implies an interface in the diffusion structure with equilibrium between three phases, either a two-phase layer adjacent to a layer consisting of a different phase (e.g. i / j interface) or adjacent two-phase layers with one common phase (e.g. k/ l interface).

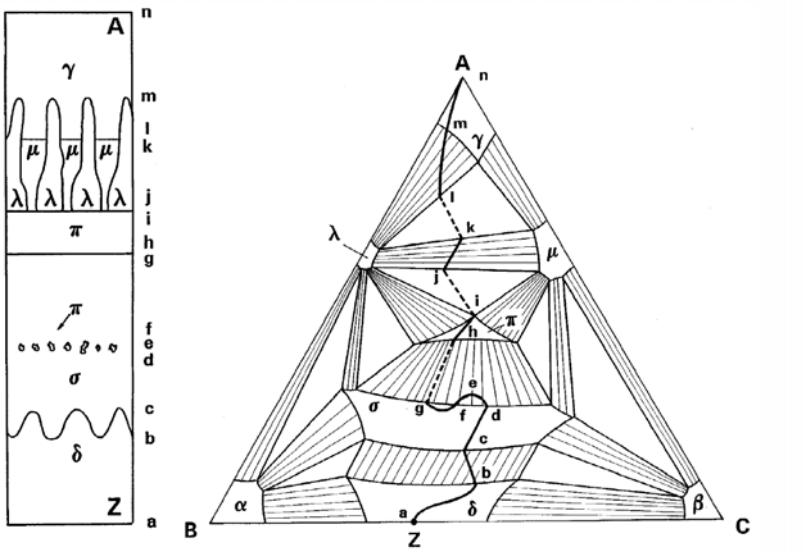

Fig. 1 A reaction zone structure in a hypothetical couple A/Z of the A–B–C system (on the left) and the corresponding diffusion path plotted on the isotherm of the ternary diagram (on the right). The low-case letters relate the structure to the appropriate composition on the isotherm. (Note: all paths in three-phase fields must be denoted by dashed lines, as a three-phase layer cannot form in a ternary diffusion couple.)

1.1.2. Preparation of diffusion couples

Several techniques are available to make solid-state diffusion couples, i.e. to bring two (or more) materials in timate contact that each diffuses into the other. In the most commonly used procedure, the bonding faces of the couple components are ground and polished flat, clamped together and annealed at the temperature of techinterest.

Depending upon the initial materials, various ambient atmospheres can be used (e.g. vacuum, inert gas, etc.). After the heat treatment, quenching of the sample is desirable in order to freeze the high-temperature equilibrium.

For some metallic systems, different electrolytic and electroless plating techniques can also be utilized to fabricate diffusion couples. In this case, one half of the couple is typically a piece of a bulk alloy. The second half of the couple is formed by plating the second alloy onto the bulk alloy substrate. Other plating techniques have also been employed including plasma spraying and chemical vapor deposition (CVD). These techniques are suitable for both metals and nonmetals. Thermal evaporation, electron beam evaporation, or laser evaporation can be used as well to deposit the second component layer onto a bulk substrate.

It is also possible to create a multiphase diffusion couple by annealing a substrate material in a reactive gas atmosphere [12]. Such experiments can be carried out in a conventional way (under isothermal conditions) or by imposing a temperature gradient perpendicular to the diffusion direction in the couple. The latter method enables one to observe competing phase reactions 'simultaneously' as a function of temperature [13].

1.1.3. Analysis methods

In order to obtain information about the phase equilibria existing in a system at a specified temperature, the phase boundary concentrations within the diffusion zone have to be measured.

Different measurement techniques can be used to determine the chemical compositions on both sides of the interfaces. There are Auger electron spectroscopy (AES), secondary ion mass spectrometry (SIMS), Rutherford backscattering spectrometry (RBS), glancing angle X-ray diffraction, electron probe microanalysis (EPMA) and analytical electron microscopy (AEM). In these methods, the last two are

the most suitable for the investigation of 'bulk' diffusion couples. The others are used for determining composition depth profiles in studies of interdiffusi0n and reactions in thin-film couples.

In the EPMA high energy electrons are focused to a fine probe and directed at the point of interest in the diffusion couple. The incident electrons interact with the atoms in the sample and generate, among other signals, characteristic X-rays. These X-rays are detected and identified for qualitative analysis and with the use of suitable standards that they can be corrected for matrix effects in order to perform quantitative analysis. In the EPMA bulk solid samples are investigated while the AEM is dealing with electron transparent thin films.

The principal advantage of the EPMA is the ability to measure compositions of very small volumes of a specimen. The spatial resolution for bulk specimens is limited to ~1μm. For thin foils, resolutions better than 50 nm are attainable routinely. Obviously, in order to obtain the most reliable results the operating conditions must be optimized. Accelerating voltage, beam current and counting time are, perhaps, the most critical parameters. The optimization of these parameters has been discussed in detail [14] and will only be summarized briefly here.

A ratio of operating accelerating voltage to excitation potential for the measured characteristic X-ray radiation of ~2-3 is desirable in order to maximize peak to background ratio and minimize the X-ray generating volume.

The value of beam current has to be chosen such that the X-ray counts are maximized for a statistically meaningful analysis without greatly increasing the electron beam size.

Counting times must be long enough to allow the accumulation of sufficient X-ray counts for statistically meaningful results (without producing too much carbon contamination).

1.1.4. Limitation and error sources

One limitation of the diffusion multiple technique is that, to avoid melting, the highest temperature for diffusion heat treatment is limited by the lowest liquidus temperature of the multicomponent system which may not be known a priori. When

liquidus is low, it may take a long time to promote sufficient interdiffusion for a reliable evaluation of properties.

The experimental results may contain errors directly attributable to the nature of the sample. One of the possible dangers of technical importance is a system in which the terminal compositions (end-members) are solids, but a liquid phase exists at the annealing temperature. It is then possible for the diffusion path to wander into this field, with disastrous results indeed! Poor adherence at the interfaces in the diffusion zone and accelerated reaction rates due to defects such as cracks, grain boundaries, etc. may also render the interpretation of diffusion couple experiments cumbersome.

Another source of error is in the experimental measurement themselves. The difficulties connected with the accurate determination of the boundary concentrations in the reaction zone are a problem for both semi-infinite and finite diffusion couple techniques. Several items concerning the electron-beam microanalytical techniques used are to be noted here.

Firstly, the determination of a chemical composition characteriswith EPMA has an inherent experimental error associated with data counting statistics and data correction procedures.

Secondly, the volume of X-ray generation in the 'bulk' samples is determined by the electron scattering in the target, and not by the incident electron beam size.

Thirdly, the X-ray absorption effect, which occurs when X-rays produced at one point within the specimen travel through materials of different compositions, and, perhaps, of different mass absorption coefficients on their way to the spectrometer. To avoid such absorption effects, it is necessary to orient the phase boundary in the diffusion couple perpendicular to the sample surface and the interphase interface parallel to the X-ray path to the spectrometer.

Finally, accurate microprobe analysis near the interfaces is sometimes very difficult owing to fluorescence effects.

1.1.5. Variations of the diffusion couple technique

There are several variations of the diffusion couple method. In the first variant, the sample to be studied is a classical semi-infinite diffusion couple, which means that after

the diffusion annealing the couple ends still have their original compositions. If volume diffusion in a semi-infinite couple is a rate-limiting step, local equilibrium is supposed to exist, in which case the rules described above can be used to relate the reaction zone morphology, developed during isothermal diffusion, to the phase diagram. The main feature of this variation of the diffusion couple method is that the phase composition of the reaction zone is independent of time and that the diffusion path is fixed. Based on diffusion couple technical, Diffusion triples (introduced by Hasebe and Nishizawa [3] for simple ternary systems and demonstrated by Jin et al. [4,5] for complex systems with intermetallic compounds) efficiently map ternary diagrams. The versatility of this technique in constructing isothermal cross-sections of ternary systems has been demonstrated repeatedly [15, 16, 17, 18].

It is often necessary to investigate couples with end members of various compositions in order to get all the information needed to find the phase relations at the annealing temperature. However, the necessary number of samples can be decreased appreciably by using polyphase terminal materials in diffusion couples. In the case of the study of, for instance, a ternary system, the chance 'to hit' interfaces at which three phases are in equilibrium, is much larger when two-phase alloys are used as end-members. Schematically this procedure is shown in Fig. 2. If a diffusion couple between P and Q is assembled, the reaction zone after annealing at a specified temperature might exhibit the morphology indicated in Fig. 2b. In area 1, microprobe measurements will reveal the three-phase equilibrium α+μ+T, whereas from area 2 the equilibrium triangle β+γ+T existing on the isotherm can be found.

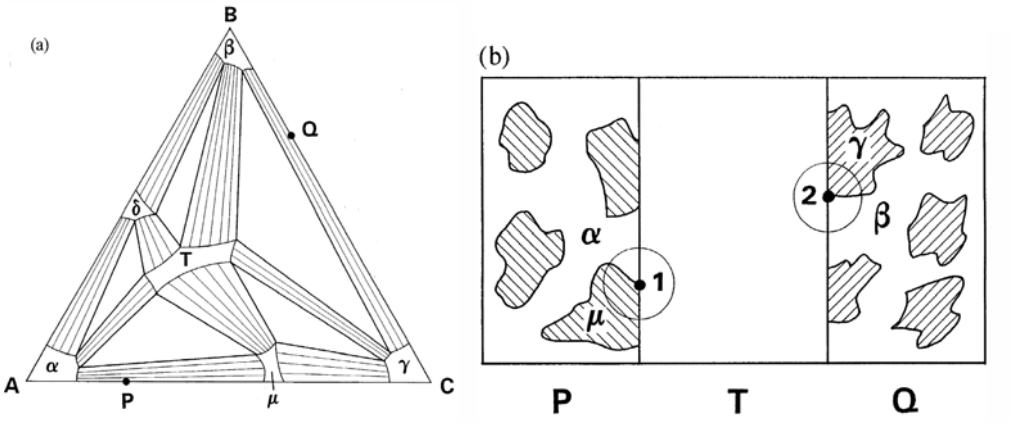

Fig. 2 Determination of the phase equilibria on the isotherm of the ternary A–B–C system using two-phase alloys as end-members (a) and schematic view of a

possible reaction zone in a hypothetical diffusion couple P/Q (b).

Further development of this technique for studying phase diagrams is connected with changing the 'macrostructure' of the classical diffusion couple. A sample is prepared by joining two plane-parallel slices of metal (alloy) through a thin layer of the third metal (alloy) as is shown schematically in Fig. 3(a). In such a layered system, in which the central part is eventually consumed, the diffusion path is not fixed as in the semi-infinite couple. The phase composition of the complex diffusion zone is changing continuously with time as a result of the overlapping of two quasi-equilibrated diffusion zones. To relate the morphology and composition of the reaction zone to the phase diagram, rules similar to those explained before still can be used. For instance, in Fig. 3 the composition found in the phases α_1 and α_2 at $t=t_3$ and t_4, respectively, are the end points of two tie-lines in the two-phase region.

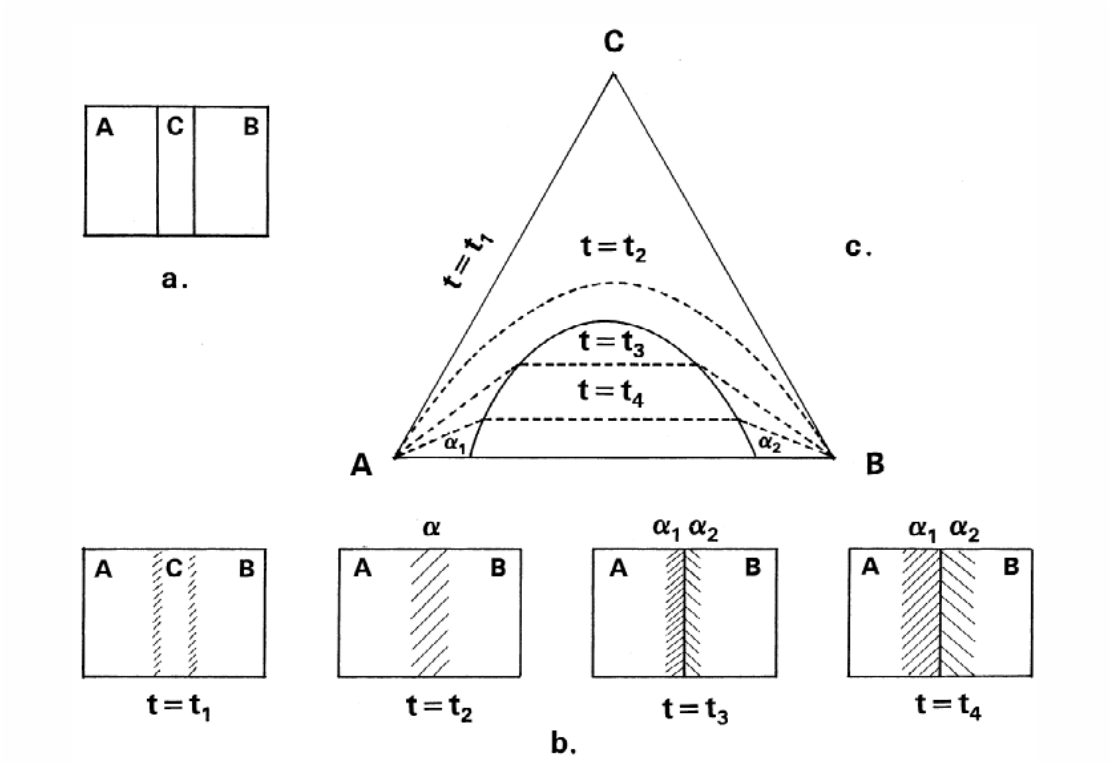

Fig. 3 Schematic view of the reaction zones and diffusion paths on an isotherm after various annealing times: (a) initial 'sandwich' sample; (b) reaction zone morphology for different annealing times; (c) diffusion paths for various annealing times.

Zhao [19] provide a high-efficiency diffusion-multiple approach and then

another [20] as shown in Fig. 4 and Fig. 5, respectively. With a diffusion couple, a series ternary systems can been investigated.

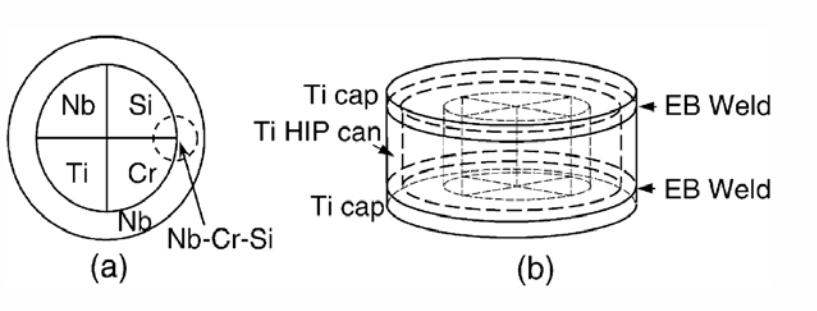

Fig. 4 A diffusion multiple for efficient determination of the Nb–Cr–Si ternary phase diagrams: (a) cross-sectional view; and (b) perspective view.

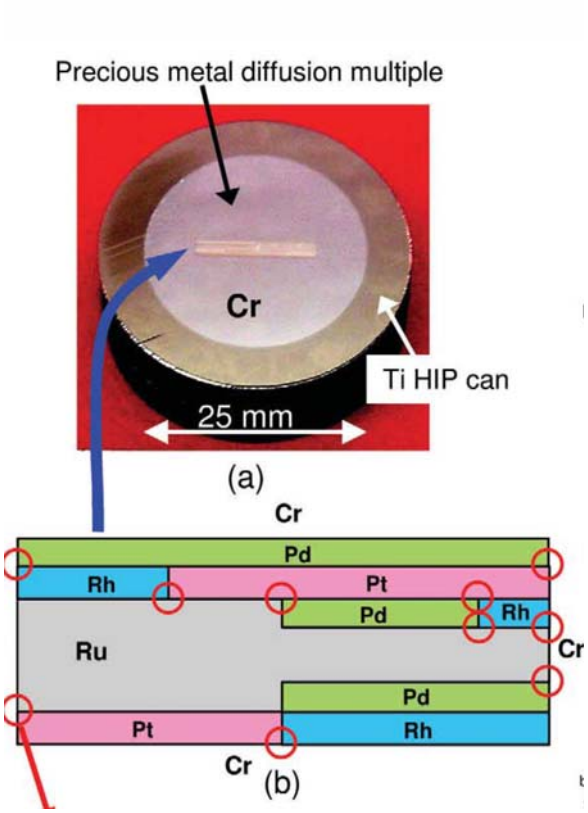

Fig. 5 Diffusionmultiple for rapid mapping of ternary phase diagrams in the Pd-Pt-Rh-Ru-Cr system. (a) Optical image of sample. (b) Arrangement of precious-metal foils to create many trijunctions (circles).

As demonstrated in the preceding sections, at an elementary level, the diffusion couple technique is nothing more than a tool for establishing a correlation between the morphology developed in the diffusion zone of the couple and a certain type of phase

relations in the system.

However, it must be added immediately that like in the case of other seemingly simple methods used in materials science, the proper use of diffusion couples for determination of multicomponent phase diagrams is by no means a trivial procedure as it might look at first sight. A number of error sources may appear when multiphase diffusion experiments are used for establishing phase equilibria.

The diffusion-multiple approach-the creation of composition gradients and intermetallic phases by long-term annealing of junctions of three or more phases/alloys-enables the study of phase diagrams, kinetics, and composition-structure-property relationships of bulk alloys [20]. It grew out of traditional diffusion couples and diffusion triples [3], which have been used to determine diffusion coefficients and phase diagrams for several decades.

In addition to mapping phase diagrams based on the local equilibriumat the phase interfaces, Zhao [21] took advantage of the fact that the thermal interdiffusion process in diffusion couples and triples can generate complete single-phase compositions of solid solutions and intermetallic compounds in binary and ternary systems. By performing localized microscale property measurements on single-phase compositions, many composition-structure-property relationships can be mapped. The term 'diffusion multiple' was coined to reflect its development from diffusion couples/triples:

1) a new sample-making process using hot isostatic pressing (HIP) allowed multiple diffusion couples and triples to be included in a single sample, thus creating a diffusion multiple;

2) localized property measurements allowed many properties to be mapped in addition to phase diagrams, thus significantly expanding the application of the methodology in materials research and discovery;

3) Diffusion couples and triples made up of multicomponent alloys were very useful for discovering new alloys, but they were no longer merely ternary diffusion couples.

Though diffusion couple technical has develop for decades of years, and has been widely used, it is still developing swiftly and violently. In a most recently presented article (actually not published yet), J-C Zhao [22] gave an overview of state-of-the-art

combinatorial/high-throughput methodologies and tools for accelerated materials research and discovery. A diffusion-multiple approach—the creation of composition gradients and intermetallic phases by long-term annealing of junctions of three or more phases/alloys—enables effective studies of phase diagrams, kinetics, and composition–structure–property relationships of bulk alloys. Such studies are made possible by localized property measurements using micro-scale probes/measurement tools. Micro-scale probes for several properties such as elastic modulus, hardness, thermal conductivity, dielectric properties, optical properties, and crystal structures are relatively well developed [20] and will be discussed in detail. The probes for electrical conductivity, magnetic properties, and compressive yield strength need further improvement or more benchmark studies. All these micro-scale probes are very useful for materials research. For instance, a micro-scale thermal conductivity probe can be used to study order–disorder transformation, site preference in intermetallic compounds, solidsolution effects on conductivity, and compositional point defect propensity. Several probes can be combined to accelerate the development of structural materials to obtain phase diagrams, diffusion coefficients, precipitation kinetics, solution-strengthening effects, and precipitation-strengthening effects. The probes yet to be developed that would have a significant impact on materials research include ones for lattice parameter measurements at micron-scale resolution, localized melting point measurements, ductility, thermal expansion coefficients, and thermodynamic properties. The impact of the development of the micro-scale probes goes beyond combinatorial materials research since most of them can be applied to non-combinatorial metallographic or thin film samples as well. Examples show that in addition to improved efficiency, the systematic nature of the combinatorial approaches can reveal complex phenomena and interactions that otherwise would be difficult to be aware of or find using conventional one-composition-at-a-time practice, especially when measurements of several properties are made using multiple probes.

The properties can be obtained through diffusion couple technical are summarized by J-C Zhao [20] as shown in Fig. 6, it is really state-of the art!

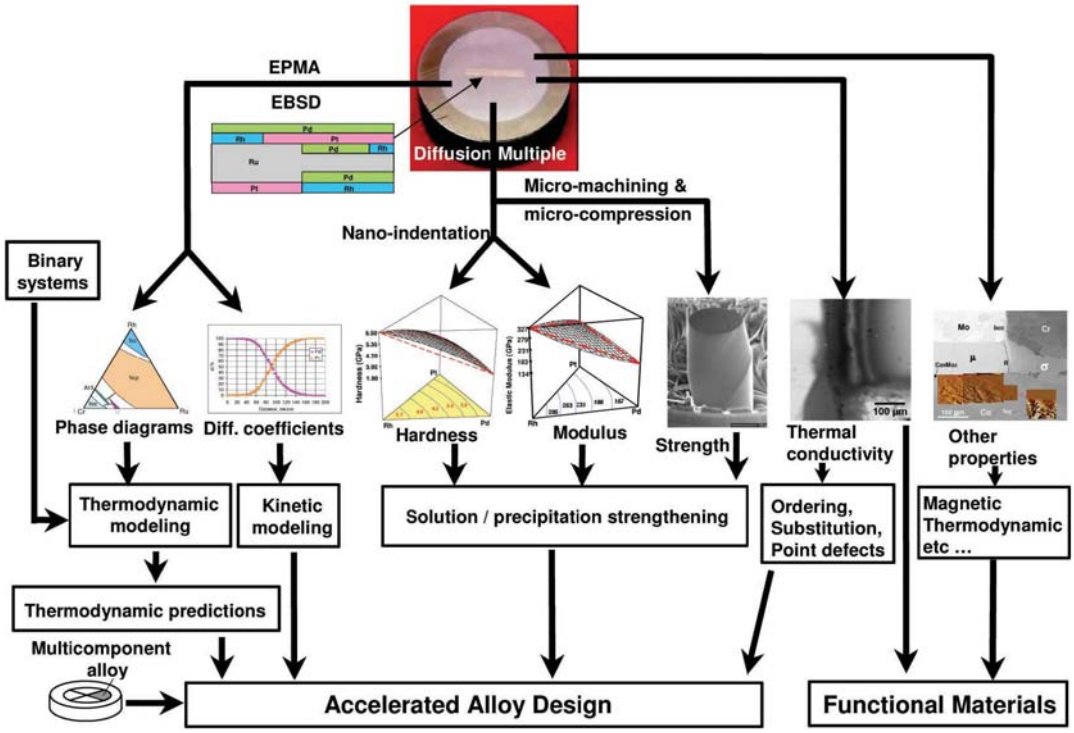

Fig. 6 Graphic summary of the diffusion-multiple approach to high-throughput materials research and discovery.

1.2. Introduction of active brazing and application of Cu-Sn-Ti system

1.2.1. General introduction of active brazing

Because of their special properties such as the ability to bear high temperatures, wear, and corrosion, ceramics have a significant potential for many structural and electrical applications, e.g. in automotive, aerospace applications [23] and so on. However, in many cases, the different ceramic parts must be connected by ceramic/ceramic joining technologies in order to fabricate complicated shapes or larger sizes. Additionally, other properties of ceramics (such as conductivity and toughness) are not comparable to those of metals. In such cases, ceramics may be joined to metals to obtain useful and stable components. As a result, the ceramic/ceramic and ceramic/metal joining technologies will be critical for the structural application of ceramics. In general, ceramic/ceramic and ceramic/metal joining have, so far, been accomplished by using a metal interlayer either by brazing or diffusion bonding [24].

Brazing is a convenient way to get a good joint. However, in either ceramic/ceramic or ceramic/metal joining, the poor wettability of conventional filler metals on ceramics is the critical problem in using the brazing method [25], because in most cases, ceramics are not wetted by molten metals [26]. The reason for this is the relatively high stability of ceramic surfaces: a ceramic/vapor interface is more stable than a ceramic/liquid interface. Therefore, in ceramic/metal (C/M) joining applications using a liquid interlayer between the ceramic and metal parts (i.e. brazing), the melt usually has to be chemically modified to promote wetting. Adding chemically active elements to the melt improves the wettability of molten metals over ceramic substrates for two reasons [27]:

1) The formation energy for the C/M interface is reduced by the negative contribution of the Gibbs free energy of the reaction between the ceramic substrate and the active alloy.

2) If the reaction product has the right properties, it will be wetted by the molten brazing alloy.

For the given reasons, to improve wettability, active elements such as titanium, zirconium, or hafnium are added to conventional filler metals, due to the chemical affinity of the active elements with the oxygen in oxide ceramics [28] or the carbon and nitrogen in carbide [29,30] and nitride ceramics [31], respectively.

Active metal brazing is a well-established technique for the joining of ceramics to themselves and to metals. In general, the active fillers can be divided into three groups, according to their melting points.

1) Low-melting-point active fillers: [32] those with a melting point below 400 ℃, a typical example being the addition of titanium to lead- or tin-based solders.
2) Medium-melting-point active fillers: [28] those with a melting point between 700℃ and 1000℃, a typical example being the addition of titanium to silver- or silver-copper-based fillers.
3) High-melting-point active fillers: those with a melting point above 1000℃, a typical example being the addition of titanium to platinum, palladium, or gold based noble-metal fillers.

Among them, the most common active filler is the eutectic 72Ag-28Cu with an addition of about 3 wt.% titanium. It has been shown that good joints can be obtained with many oxide and nonoxide ceramics by using these kinds of active fillers [28~31]. However, the interfacial thermal stress generated due to the difference in thermal-expansion coefficients of the ceramic and metal during the cooling process after brazing might deteriorate the joints. To solve this problem, low melting-point active fillers have been developed. Although the brazing was also conducted at higher temperatures, the active fillers solidified at lower temperatures, which effectively alleviated the thermal stress between ceramic and metal.

Okamoto indicated in a review article that interracial reactions are unavoidable in most metal-ceramic joining [24]. The formation of interfacial phases affects the wetting process and the joining strength of the brazed ceramic components. However, Chung and Iseki demonstrated that the joining of ceramics could be accomplished by adsorption of the Ti element on the interface, regardless of whether an interfacial reaction layer was formed [33]. For the brazing of $A1_20_3$, SiC, and Si_3N_4 with AgCuTi active fillers, many research efforts have shown that the Ti in active fillers can react with Al_2O_3, SiC, and Si_3N_4 to form titanium oxides [34,35], titanium silicides, titanium carbides [36], and titanium nitrides [31], respectively.

1.2.2. Application of Cu-Sn-Ti

Brazing diamond grits onto a steel substrate in the form of a single-layer configuration has been deemed as an effective route to the manufacturing of high-performance diamond abrasive tools[37]. When compared with electroplated diamond tools, it is possible to expose higher protrusion heights of diamond grits above the level of the brazing alloy but still achieve stronger adhesion strength between the diamond grits and the brazing alloy. Such a unique characteristic can yield diamond abrasive tools exhibiting higher material removal rates as well as longer tool lives. The success of brazing the diamond grits onto the steel substrate depends on the adhesion strength between the diamond grits and the brazing alloy, which is usually enhanced by the incorporation of active elements, such as Ti, Cr, V, and Zr, into the brazing alloy [38,39]. These active elements can easily develop interracial compounds with the diamond grits during the brazing operation, which can alleviate the interfacial stress caused by the different crystallographic lattices and thermal-expansion coefficients

between the diamond grits and the braze matrix. Among various systems, alloys composed of Ag, Cu, and a low concentration of active Ti (less than 5 wt pct) are commonly used as the brazing alloys for the diamond [37,40,41] and the other ceramic materials[42,43,44].

When Ti was used as an active element, the interaction between the Ti and diamond determines the interfacial microstructure, which imparts a strong effect on their interracial adhesion strength. Since the free energy of formation of TiC is about -171 kJ/mol at 925℃, the interfaces between the brazing alloy and the diamond grits are thermodynamically stable sites for the Ti atoms to diffuse to during the brazing operation. In fact, segregation of Ti atoms to the interfacial area was widely recognized in several prior reports, not only in the brazing of diamond [45], but also in the brazing of various oxide[42,43], carbide [46], and nitride [44] ceramic materials. Such interfacial layers were widely recognized to be beneficial to the adhesion strength between the braze matrix and the ceramic materials. Nevertheless, excessive development of the interfacial reaction layers can lead to the formation of defects, which inevitably impart weakening to the bond.

Although alloys based on Ag, Cu, and Ti are widely used for the brazing of diamond grits onto a steel substrate, these alloys are low in strength and wear resistance and are not suitable for fabricating diamond abrasive tools of a single layer configuration. Different alloys, such as those composed of Ni, Fe, and Cr, are, thus, the alternatives. Nevertheless, these elements tend to catalytically convert diamond into graphite at high temperatures and, thus, deteriorate the strength of diamond. The other alternative is to reinforce the brazing alloys by the incorporation of reinforcing phases. Reinforcing phases, such as Si3N4, TiC, SiC, WC, W, and Mo, show positive results in terms of abrasion resistance and tool life [47]. The problem associated with such an approach is that the relative volume fraction of the reinforcing phase must be limited, in order to maintain a sufficiently high quantity of liquid phase during the brazing operation.

Alloys based on Cu-Sn-Ti are effective alternatives to Cu-Ag-Ti alloys for the processing of single-layered brazed diamond tools and metal-bonded diamond tool bits [47]. Both tool life and cutting speed have been increased. Up to now Cu-Sn-Ti filler metals show the best combination of properties, especially due to their relatively high

strength and erosion resistance if compared to Ag-Cu alloys and their lower melting point if compared to Ni-base ones [48]. In general, tool performance is dictated by the bonding strength between the abrasive grits and the braze matrix and the mechanical properties of the braze matrix, both of which depend on the microstructure of the brazed structure. Substitution of Sn for Ag resulted in different phase-partitioning phenomena. For example, the activity coefficient of Ti in the Cu-Ag-Sn-Ti (Ag: 72 to 100 wt pct, Sn: 0 to 10 wt pct) increased with increasing Ag concentration but decreased with increasing Sn concentration in the liquid state. In other words, in the concentration range defined, the concentration of Ti dissolving in Cu-Ag-Sn-Ti alloys decreased with increasing Ag concentration, but increased with increasing Sn concentration. The addition of Sn not only could reduce the melting temperatures of these alloys, but also could promote the dissolution of a higher concentration of Ti into the liquid phase. The coexistence of high concentrations of Sn and Ti in the liquid phase can possibly cause precipitation of reinforcing Sn-Ti intermetallic phases in the braze matrix during cooling. Based on the previous analyses, the alloying concentration of Ti in the brazing alloy can be increased and the hardness of the braze matrix can be enhanced with the substitution of Sn for Ag [49].

Chapter 2. Interfacial reactions of Cu-Sn-Ti boundary binary systems

2.1. Introduction

The formation of intermetallic compounds at the inter face during bonding plays an important role in the wettability and the mechanical properties.

If these interface reaction products between substrate and various solder alloys can be predicted, it would be helpful to an understanding of the physical metallurgy of the substrate/solder joint as well as to designing new multicomponent solder.

Based on the idea that no element can intrinsically diffuse in a direction in which its own chemical potential is increased, Van Loo [2] developed a model for the prediction of intermetallic compounds in metal-ceramic combinations. This model can also be applied to the case of the substrate/solder interface reaction if the mutual solubility of each phase is small. When more than two intermetallic compounds are formed at the interface, the layer sequence between the substrate and the solder can be predicted using this model. However, this model does not give any information as to which compound would form first during the soldering process among various possible compounds. Since only the intermetallic compound that forms first during the soldering process would have an effect on the wettability of solder, it would be important to predict such a compound.

B.J. Lee [50] suggests a new scheme to predict the intermetallic compound that forms first at the substrate/solder interface during the soldering process. The key idea is that the composition at the substrate/solder interface can be estimated by calculating metastable equilibria between the substrate and the liquid solder phases. Under the metastable equilibrium state, the compound which has the highest driving force of formation can be selected as the compound that would form first during the soldering process. In order to predict which compound will form first, the nucleation activation

energy for each compound should be compared. The nucleation activation energy depends on the driving force and the interface energy, but information on the interface energy is lacking. Besides, the interface energy, which is experimentally determined based on the macroscopic concept, tends to be modified for a smaller cluster such as the critical nucleus. For practical purposes, the driving force can be an approximate criterion to predict the first-forming compound.

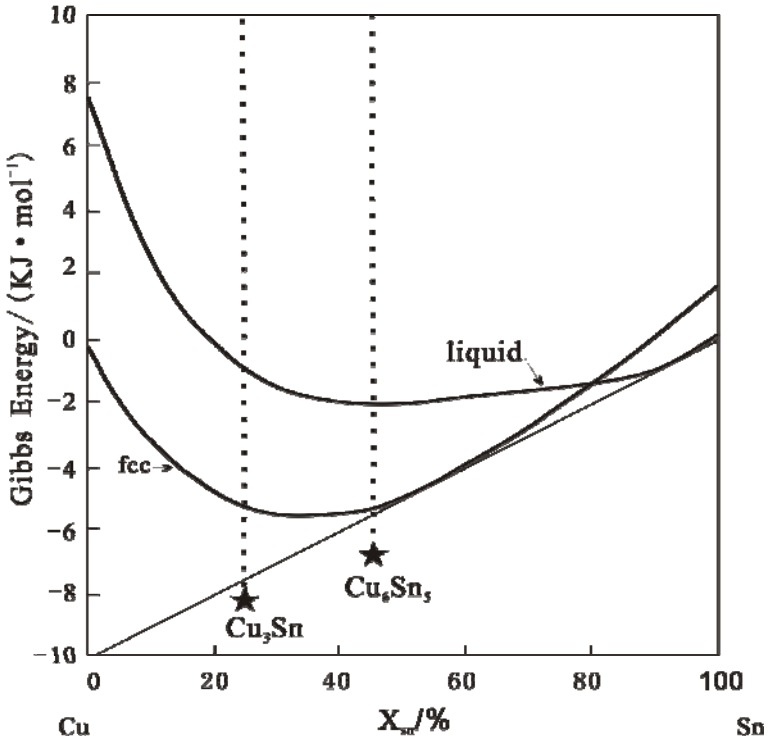

Fig.7 Illustration of driving forces of formation for Cu_3Sn and Cu_6Sn_5 under metastable equilibrium between fcc-Cu and liquid at 250℃ in Cu-Sn binary system. The thick lines are the Gibbs energy curves of fcc-Cu and liquid， the thin line is the common tangent for the two curves. The Gibbs free energy of Cu_3Sn and Cu_6Sn_5 are denoted by "*". The difference between the common tangent curve and the Gibbs energy of Cu_3Sn or Cu_6Sn_5 at the same X_{Sn} values correspond to the driving forces of formation of the either phase, respectively.

2.2. Experimental procedure

2.2.1. preparation of Sn/Ti liquid/solid diffusion couples

Ti plate (99.9 wt. %) and Sn ingot (99.999 wt. %), were used as starting materials.

Small pieces of Sn and Ti were cut off and the surfaces of each piece were polished metallographically and cleaned with ultrasonic. Each pair of Sn and Ti was sealed in an evacuated quartz tube filled with argon (to avoid floating of Ti in molten Sn, Ti pieces were fixed in the tubes with Mo wires).

Place the tubes into annealing furnace vertically, subsequently rise the temperature to 873K and make Sn pieces molted. Shake the tubes to make Ti pieces merged into molten Sn and Sn/Ti liquid/solid diffusion couples were obtained. The tubes were kept at 873K for 30 and 160 mins.

2.2.2. preparation of Cu/Sn solid/liquid diffusion couples

Cu plate (99.97 wt. %) and Sn ingot (99.999 wt. %), were used as starting materials. The diffusion couples were made with the similar progress as making Sn/Ti diffusion couples. The annealing temperature was 808K, and the annealing time were 10, 30 and 60 mins respectively.

2.2.3. preparation of Cu/Ti diffusion couple

Cu and Ti pieces of 5mm* 8mm were cut off and diffusion welded at 1023K, 4MPa pressure for 15 mins, sealed in an evacuated quartz tube filled with argon and annealed at 1023K for 1000h.

The tubes were quenched in water and broken. The taken out samples were mounted, grounded and polished metallographically. Then the samples were analyzed with Scanning Electronically Microscope (SEM) and EPMA (JEOL JXA-8800R), in order to determine the formed intermetallic compounds.

2.3. Results and discussion

2.3.1. The first phase forms in Ti/Sn diffusion couple

Fig.8 show the backscattered electron (BSE) images of Ti/Sn diffusion couples annealed at 873K. The EPMA result shows there is only Sn_3Ti_2 forms at the interface.

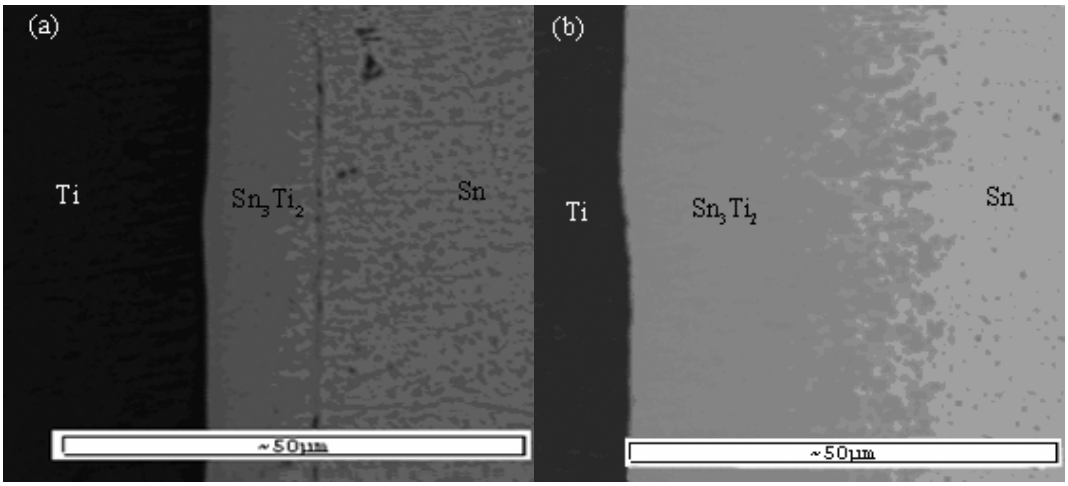

Fig.8 The backscattered electron (BSE) images of Ti/Sn diffusion couples annealed at 873K.

(a)-30mins; (b)-160mins

Based on the former literature [51], Kuper found a new binary phase Sn_3Ti_2. Based on work of workgroup member Liu Chunlei's work, the author reevaluated the Ti-Sn binary phase diagram, as shown in **Fig.9**

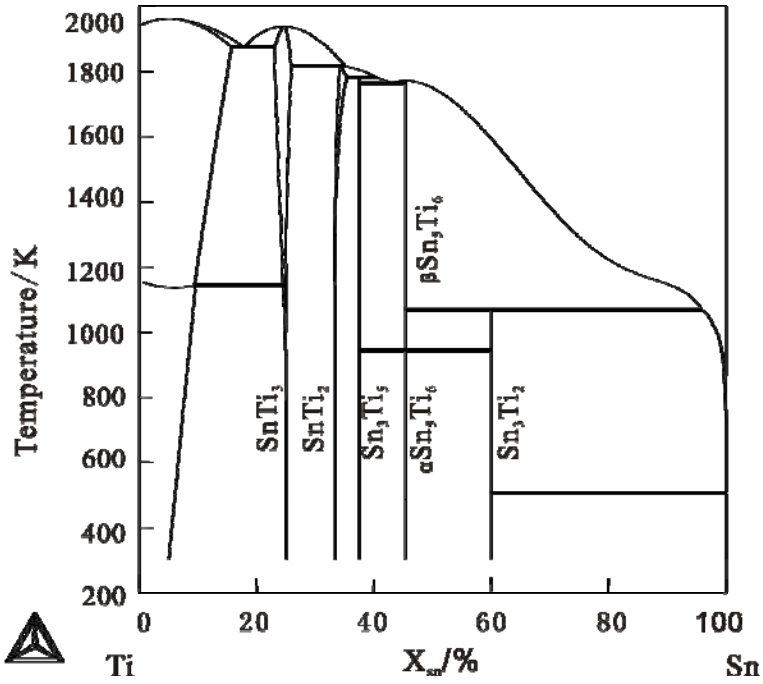

Fig.9 caculated Sn-Ti binary phase diagram

From Ti-Sn binary phase diagram, there are five binary compounds, $SnTi_3$, $SnTi_2$, Sn_3Ti_5, Sn_5Ti_6 and Sn_3Ti_2, exist stably at 873K

Table 1 The formation driving force of the intermetallic compounds under the metastable equilibrium of hcp(Ti)+liq(Sn) at 873K

metastable equilibrium	hcp(Ti)+liquid(Sn)				
phases stable at 873K	Sn_3Ti_2	Sn_5Ti_6	Sn_3Ti_5	$SnTi_2$	$SnTi_3$
driving force(KJ/mol)	4996.27	3242.93	1847.19	211.21	-897.10

The formation driving force of the intermetallic compounds under the metastable equilibrium of hcp(Ti)+liq(Sn) at 873K are listed in Table 1.

As can be seen in Table 1, at 873K, under the metastable equilibrium state of hcp(Ti) and liquid, the phase with the highest formation driving force is Sn_3Ti_2. According to largest driving force criteria, the first forming phase should be Sn_3Ti_2, and the theoretical calculated results agree well the experiment results.

2.3.2. The formation sequence in Cu/Sn diffusion couples

Fig.10 shows the morphology of Cu/Sn solid-liquid diffusion couples anneals at 808K. From **Fig.10**, it can be seen that after annealing for 10 mins, there is only Cu_3Sn forms in the couple. With the annealing time increasing to 30 mins, $Cu_{41}Sn_{11}$ appears in the diffusion layer between Cu and Cu_3Sn. After annealing for 60 mins, another phase bcc-a2 between Cu and Cu_3Sn can be detected.

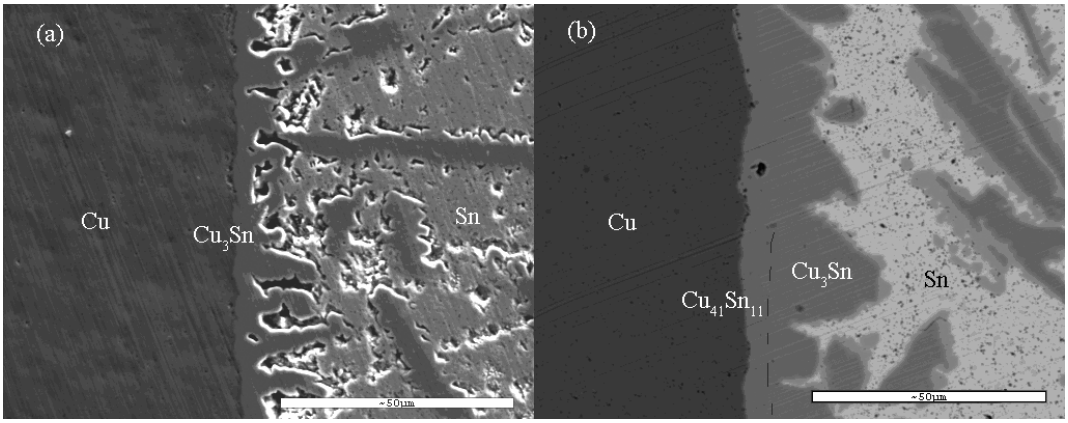

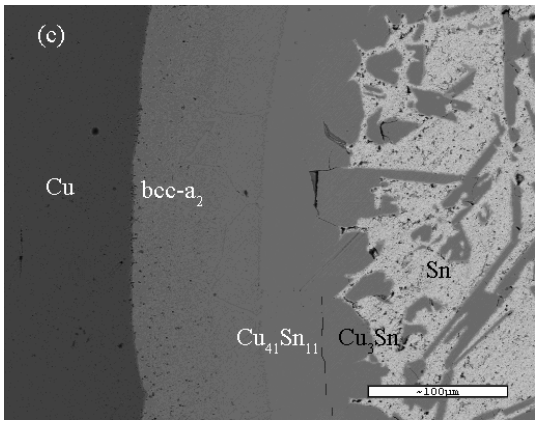

Fig.10 BSE image of Cu/Sn diffusion couple annealed at 808K. The type of phase are detected with EPMA. The interface between $Cu_{41}Sn_{11}$ and Cu_3Sn are indicated in dashed lines.

(a)-10mins；(b)-30mins；(c)-60 mins

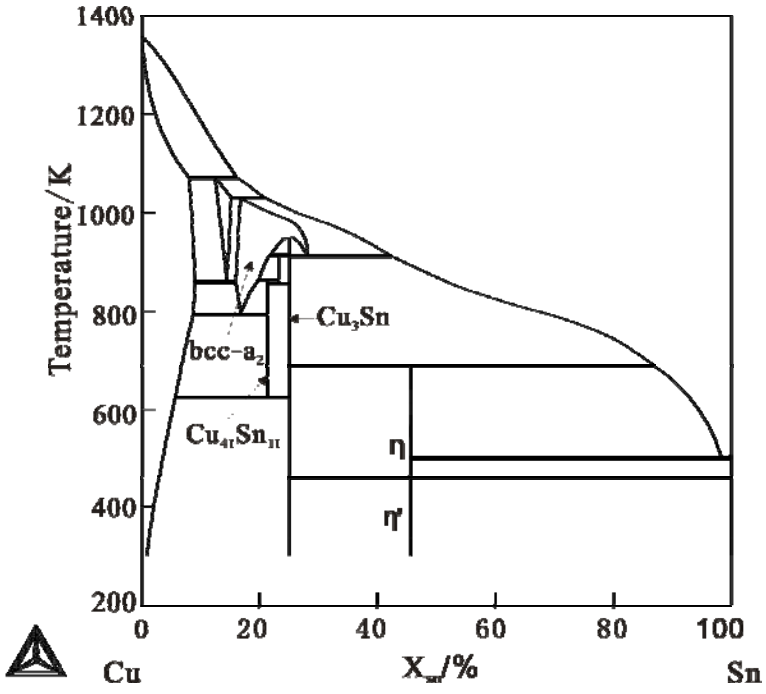

Fig.11 Cu-Sn binary estimated by Shim [52].

In this work, the thermodynamic parameters estimated by Shim [52] is applied for calculating. The calculated Cu-Sn binary phase diagram is shown in **Fig.11**. From Cu-Sn binary phase diagram, the phases exist stably at 808K are Cu_3Sn, $Cu_{41}Sn_{11}$ and Bcc_a_2. There formation driving force are listed in **Table 2**.

Table 2 The formation driving force of the intermetallic compounds in Cu-Sn

system at 808K.

Phase	Driving force (J/mol)		
	Cu+liquid(Sn)	Cu+ Cu_3Sn	Cu+ $Cu_{41}Sn_{11}$
Cu_3Sn	105.01	0	-151.22
$Cu_{41}Sn_{11}$	-977.44	114.12	0
Bcc_a_2	-202.32	104.51	31.69

As can be seen in **Table 2**, under the metastable equilibrium state of liquid and fcc-Cu, the phase with the highest driving force of formation is Cu_3Sn. According to largest driving force criteria, the first formatting phase should be Cu_3Sn, and this can be seen in **Fig.10**(a). According to essential rules of thermodynamics and diffusion couple approach, formation of any phase must combining with decrease of Gibbs Energy, it means phases with negative driving force cannot form. However, after Cu_3Sn appearing, diffusion couple made of Cu and Cu_3Sn are obtained. According to the driving force of other phases under metastable equilibrium Cu+Cu_3Sn, which are listed in **Table 2**, both formation driving forces of $Cu_{41}Sn_{11}$ and Bcc_a_2 are positive and that of $Cu_{41}Sn_{11}$ is larger. Therefore, after Cu_3Sn, the second phase forms in diffusion couple should be $Cu_{41}Sn_{11}$ and the phase appears at last should be Bcc_a_2. As illustrated in **Fig.10**(b) and (c), the theoretical calculated results agree well with the experiment results.

2.3.3. The phase absent in Cu/Ti diffusion couple

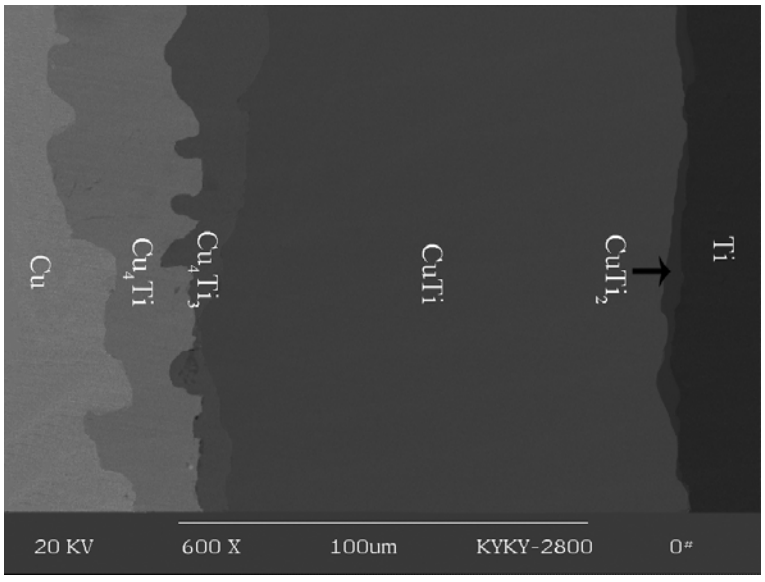

Fig.12 BSE image of Cu/Ti diffusion couple annealed at 1023K for 1000 hours.

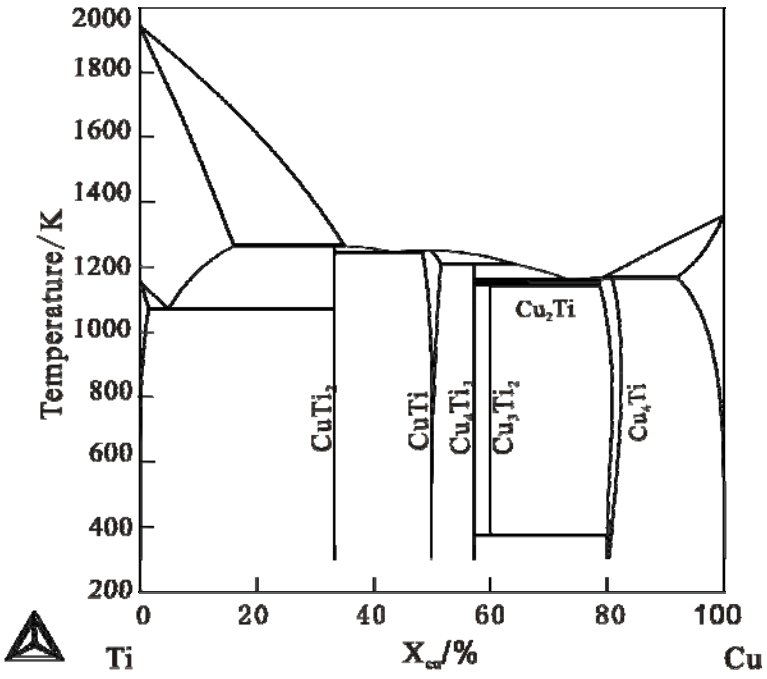

Fig.13 Cu-Ti binary phase diagram evaluated by Kumar [53].

Fig.13 shows the Cu-Ti binary phase diagram evaluated by Kumar [53]. From the phase diagram, it can be seen there are 5 stable binary compounds in this system at 1023K. However, **Fig.12** shows the morphology of Cu/Ti diffusion couple annealing at 1023K for 1000h, there are four compounds $CuTi_2$, CuTi, Cu_4Ti_3, Cu_4Ti_3, appears in the sample, while Cu_3Ti_2 is absent.

To explain the reason that Cu_3Ti_2 does not appear when all other stable phase exist, the formation driving force of intermetallic compounds are calculated and listed in **Table 3**. Meanwhile, the metastable have no relations with this experiment result are not given.

Table 3 The forming driving force of the intermetallic compounds in Cu-Ti system at 1023K

Phase	Driving force (KJ/mol)		
	fcc(Cu)+hcp(Ti)	fcc(Cu)+ $CuTi_2$	fcc(Cu)+ Cu_4Ti_3
$CuTi_2$	5528.09	0	-4889.85
CuTi	3553.86	2834.40	-699.41

Cu_4Ti_3	1725.91	3069.65	0
Cu_3Ti_2	809.34	2977.70	126.48
Cu_4Ti	-2608.37	1998.27	724.38

Combining Cu-Ti binary phase diagram and **Table 3**, we can deduce the reacting process of Cu/Ti diffusion couple is in this way. At 1023K, under the metastable equilibrium of fcc(Cu)+hcp(Ti), the phase $CuTi_2$ with maximum formation driving force forms firstly. According the binary phase diagram, the equilibrium between Ti and $CuTi_2$ is stable (there is no other stable phase between them), so the equilibrium will no longer being considered. The next step should be considering the metastable equilibrium Cu+$CuTi_2$ and the intermetallic phase with largest driving force is Cu_4Ti_3. Once Cu_4Ti_3 forms between Cu and Cu_4Ti_3, other two metastable equilibria appear. Because the composition of Cu_3Ti_2 locates between Cu and Cu4Tui3, and the compound, $CuTi_2$, between $CuTi_2$ and Cu_4Ti_3 has formed in the sample, there is only one metastable equilibrium, Cu+Cu_4Ti_3, needs further study. As indicated in **Table 3**, the two phases between Cu and Cu_4Ti_3 are Cu_3Ti_2 and Cu_4Ti, and both of them have positive driving force. However, the formation driving force of Cu_4Ti is larger than that of Cu_3Ti_2. Until now, it is explain theoretically that Cu_3Ti_2 is the phase forms at last in Cu-Ti binary system. In addition, it is the very reason for the absence of Cu_3Ti_2 when all of $CuTi_2$, CuTi, Cu_4Ti_3 and CuTi appear.

2.4. Conclusion

Only Sn_3Ti_2 forms if Ti/Sn solid/liquid diffusion couples are annealed at 873K for 30~160 mins.

When annealed at 808K for 10 mins, only Cu_3Sn forms in Cu/Sn solid/liquid diffusion couple. With the annealed time increasing, $Cu_{41}Sn_{11}$ layer forms between Cu and Cu_3Sn in 30 mins, and then bcc-a2 layer forms between Cu and $Cu_{41}Sn_{11}$ in 60 mins.

After annealing at 1023K for 1000 hours, four compounds, $CuTi_2$, CuTi, Cu_4Ti_3 and Cu_4Ti_3 form in Cu/Ti diffusion couple while Cu_3Ti_2 is absent.

The interfacial reaction process and phase formation sequence has been predicted with the maximum driving force model using Thermo-Calc software.

Chapter 3. Phase Relations in the Cu-Sn-Ti Ternary System at 823K Determined by Diffusion Triple Technique

3.1. Introduction

Cu-Sn-Ti alloys are effective braze for diamond tools and metal-bonded diamond tool bits [47]. Copper rich Cu-Sn-Ti alloy is also used as binder for liquid phase sintering of diamond tools [54]. For example, Cu-10Sn-15Ti [49] (wt.%) alloy is used in bonding diamond grits to steel substrates and fine structure in the brazing area has been obtained. In order to further improve the performance of brazing structures, more suitable process of brazing may be an efficient way. Phase diagrams of the related system can provide a guideline to achieve this purpose and to develop new series of such solders. However, there is little information available on the Cu-Sn-Ti phase diagram. Naka et al. [55] have determined the liquidus of this system. Three ternary intermetallic compounds were reported: $CuSn_3Ti_5$ [56]with Ti_5Ga_4 structure [57,58], Cu_2SnTi [59] with a cubic structure and CuSnTi[58] isostructural to $InNi_2$ [60]. No isothermal section has been established.

Information of isothermal section would be very time-consuming and expensive to obtain using the conventional one-alloy-at-a-time approach. As an effective alternative, diffusion triple [3,4,5] approach has been widely used to efficiently map the ternary phase diagrams of solid material systems. The purpose of this work is to measure phase relations of the Cu-Sn-Ti ternary system at 823K with the solid/solid/liquid diffusion triple.

3.2. Experimental Procedure

Sn ingot (99.999 wt. %), Cu plate (99.97 wt. %) and Ti plate (99.9 wt. %) were

used as starting materials. Small pieces of Cu and Ti were cut off from respective plates and the surfaces of each piece polished metallographically. Each pair of Cu and Ti was diffusion welded at 973K for 10 mins in argon flow, and then sealed in an evacuated quartz tube filled with argon, subsequently annealed at 1023K for 1000 hours in a diffusion furnace and finally quenched in air. According to Cu-Ti binary phase diagram [53], no reaction occurs between 823K and 1023K, and compositions of Intermediate Compounds (IMCs) do not much change in this temperature range. Thus taking Cu-Ti couple from 1023K to 823K will not affect the results.

To prepare Cu-Ti/Sn diffusion triples, each Cu-Ti couple was encapsulated in a quartz tube filled with pure argon. The diffusion couple was fixed by molybdenum wire and kept parallel to the tube, with a piece of Cu 20 wt.%-Sn ingot prepared afore. Note here we use Cu 20 wt.%-Sn solution instead of pure Sn as the terminal component in preparing diffusion triple in order to compensate the loss of Cu due to the quick dissolution of Cu into molten Sn [61]. The capsules were vertically placed in a box-type furnace and annealed at 823K. At 823K, Cu-Sn solution was melted and then surrounded the Cu-Ti couples to form the Cu-Ti-Sn solid/solid/liquid diffusion triples. The assembling procedure is illustrated in Fig.14. After kept at 823K for 30 to 480 mins, the tubes containing the diffusion triples were taken out of the furnace and water-quenched.

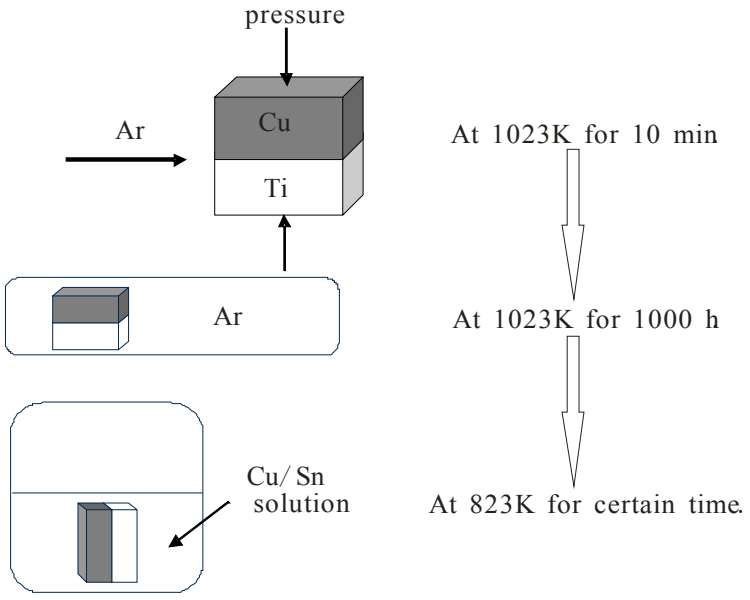

Fig.14 The scheme of assembling process of diffusion triple

The obtained triples were mounted, grounded and polished using standard metallographic techniques for subsequent analysis. Microstructures of diffusion triples were examined by Scanning Electron Microscopy with Energy Dispersive Spectrometry (SEM/EDS) and phase compositions were measured by quantitative EPMA analysis on a JEOL JXA-8800R (Japan Electron Optics Ltd., Tokyo, Japan) microprobe with 20kV, 20nA and 40°take-off angle, respectively. To determine the tie-lines of the two adjacent phases, composition profiles along the lines perpendicular to the corresponding interfaces were measured and extrapolated.

3.3. Results and Discussion

3.3.1. Morphology of Diffusion Triple

Phases and their contacting relations in the triples annealed for 30 to 480 mins are the same. The backscattered electron (BSE) images of the Cu-Sn-Ti diffusion-triple annealed at 823K for 480 mins are illustrated in Fig.15. Fig.15(a) shows the panorama view of diffusion triple. Partial of Cu and Cu-Ti compounds have dissolved into liquid matrix, and IMCs formed on the interface between liquid and Cu-Ti diffusion couple. Fig.15(b), (d), (e), and (g) are magnified parts in Fig.15(a). Fig.15(b) keeps the morphology of Cu-Ti diffusion couple where four layers of Cu-Ti binary IMCs, $CuTi_2$, CuTi, Cu_4Ti_3, and Cu_4Ti formed at 1023K showed clearly, but Cu_3Ti_2 was not detected. Fig.15(c) shows details near Ti matrix with two phases Sn_5Ti_6 and Sn_3Ti_2. Sn_5Ti_6 contacts with both $CuTi_2$ and CuTi. There are Cu_3Sn and Sn_3Ti_2 crossing with each other. At lower part of Fig.15(c), a ternary phase CuSnTi is detected near the interface of CuTi. In order to see this interface more clearly, an enlarged image was taken as shown in Fig.2(d). As indicated in Fig.2(d), it is Sn_5Ti_6 rather than CuSnTi keeps contact with CuTi phase. Fig.15(e) shows details near the Cu matrix. In this region, three Cu-Sn binary phases, Bcc_a_2, $Cu_{41}Sn_{11}$ and Cu_3Sn, form between pure Cu and liquid matrix. Layer-type CuSnTi was also found between Cu_4Ti and Cu-Sn binary compounds and it extend into the region between Bcc_a_2 and Cu matrix. Sn_3Ti_2 grows between liquid and Cu_3Sn/CuSnTi. The dash line between the Cu-Sn binary compounds is drawn according to the EPMA results and shows the phase boundaries. These phase boundaries are almost invisible in BSE image due to their similar average atomic weights. As shown in Fig.15(f), most of the CuSnTi phase exists as dispersive

particles between Cu-Ti and Cu-Sn binary compounds. Clearly, CuSnTi is in equilibrium with each Cu-Sn binary compound. Tri-phase junction among Cu_4Ti_3, CuSnTi and Sn_5Ti_6 can also be found in Fig.15(f). All the phases in Fig.2 are determined by the composition measured by EPMA.

According to Hamar-thibault [58], $CuSn_3Ti_5$ is not stable at 823K. Neither Hamar-thibault [58] nor Naka55 found Cu_2SnTi at entire temperature range in their work and the original data of Heine [59] gave no information about the condition that Cu_2SnTi existing stably. Meanwhile, Cu_2SnTi is not detected and is not considered in this work. Therefore, CuSnTi is the only stable ternary compound in Cu-Sn-Ti system at 823K and it appears in the diffusion triple.

According to the Cu-Ti, Sn-Ti [51,62] and Cu-Sn [52] binary phase diagrams, Cu_3Ti_2, $SnTi_3$, $SnTi_2$ and Sn_3Ti_5 do not present in this experiment.

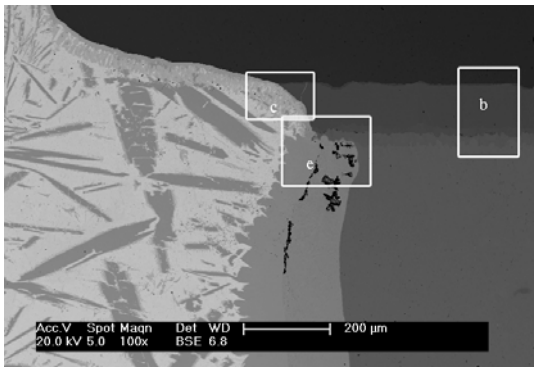

a

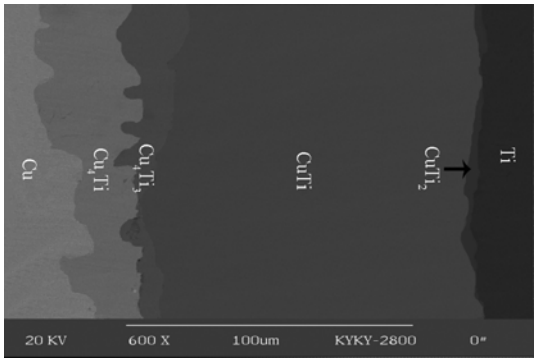

b

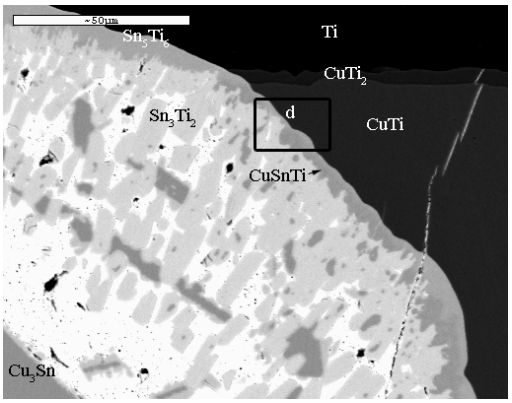

c

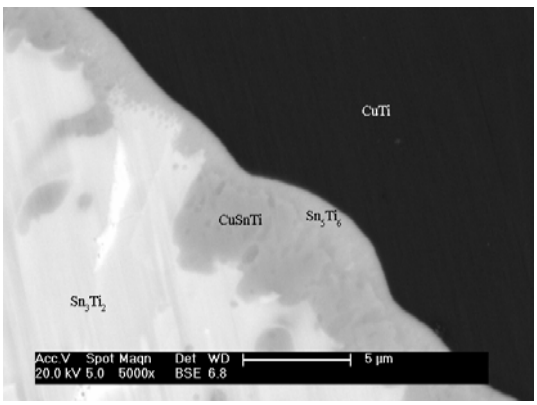

d

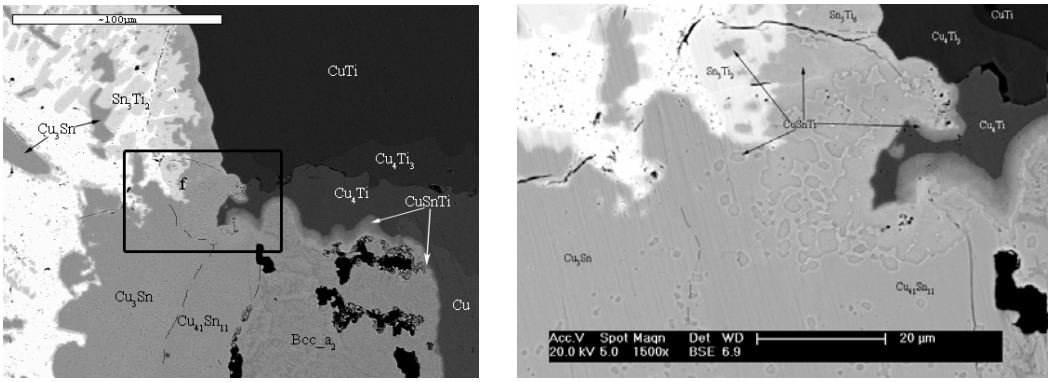

e f

Fig.15 BSE images of diffusion triple annealing at 823K for 480 mins. (a) panorama view; (b), (c), (e) and (g) magnified images in areas marked in (a); (d) and (f) are magnified images in areas marked in(c). and (e), respectively.

3.3.2. Phase Relations among Sn_3Ti_2, Cu_3Sn, CuSnTi, and liquid

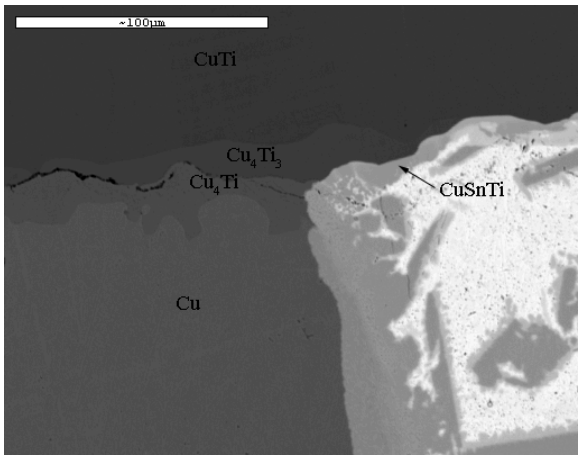

Fig.16 BSE images of diffusion triple annealing at 823K for 60 mins.

As shown in Fig.15(c) and Fig.15(f), Cu_3Sn is adjacent with Sn_3Ti_2, it seems that they are in equilibrium at 823K with each other. In order to clarify if such equilibrium is real or not, let us have a look at the microstructure of the Cu-Sn-Ti diffusion-triple annealed at 823K for 60 mins (Fig.3). Comparing the phase distribution in Fig.3 with that in Fig.2, we can know that phase relations do not change except the connection between CuSnTi and liquid is clearer. This indicates the equilibrium between CuSnTi and liquid. The tie-line corresponding to such equilibrium will overlap and cross with

the tie-line between Cu_3Sn and Sn_3Ti_2 in the same isothermal section (See Section 3.3.4). Obviously, the simultaneous existence of these two tie-lines breaks the phase rule, and only one of these two tie-lines can be stable at 823K.

Now let us analyze the morphology and distribution of the involved phases (Sn_3Ti_2, Cu_3Sn, CuSnTi, and liquid). CuSnTi in the triple for 60 mins (Fig.16) must form during annealing because of its considerable size. Furthermore, as shown in Fig.2 and Fig.16, CuSnTi block presents at similar place, next to Cu_4Ti_3. This implies that the tie-line between CuSnTi and liquid is more acceptable. Firstly, though both Cu_3Sn and Sn_3Ti_2 are stable phases at 823K, part of the can also form during quenching. It is worth noting that there are two types of morphology for Sn_3Ti_2. One is compact layer locates next to Sn_5Ti_6 and the other is incompact particles next to liquid. The compact part of them should be formed during annealing process, the incompact one formed during quenching. Similar case happens to Cu_3Sn too. Secondly, solubility of Cu and Ti in liquid Sn at 823K can be up to 40 at.% [52] and nearly 10 at.% [51,62], respectively. Considering the original Cu content in Sn solution (20 wt.%)， consummation of both Cu-Ti binary compounds and pure Ti, measurable Cu and Ti should solute in liquid. However, in the obtained sample, the content of Cu and Ti in Sn is only about 2~3 at.% and less than 0.5 at.%, respectively. To fulfill the conservation of mass, certain amount of Sn_3Ti_2 and Cu_3Sn precipitating from liquid in cooling process is necessary. Because the certainty of dispersion of Sn_3Ti_2 and Cu_3Sn with temperature decreasing, it is highly possible that they contact together when quenching. So Cu_3Sn and Sn_3Ti_2 contacting with each other in Fig.2 must be the solidification products during quenching. Hence, a conclusion is drawn that CuSnTi and liquid are in equilibrium with each other, and two three-phase equilibria, liquid+Sn_3Ti_2+CuSnTi and liquid+CuSnTi+Cu_3Sn, exist in the area surrounded by liquid, Sn_3Ti_2, CuSnTi and Cu_3Sn at 823K.

3.3.3. Determination of the tie-line between CuSnTi and the Cu-Sn Compounds

As indicated in Fig.15(f), in addition to appear in Cu-Ti and Cu-Sn binary compounds, we also find many dispersed CuSnTi particles also exist in the Cu-Sn binary compounds. The phase boundaries between CuSnTi and Cu-Sn binary compounds have very complex morphology with well dispersed fine particles which

are difficult to analyze by EPMA.

In order to determine their tie-lines, data obtained in these two phase region are dealt with following approach:

We first treat CuSnTi as a stoichiometric phase with Cu:Sn:Ti ratio equals to 1:1:1 and note that Ti solubility in all of Cu-Sn binary compounds is negligible, now assuming the composition determined by EPMA is $x_{Cu} : x_{Sn} : x_{Ti}$, then $(x_{Cu} - x_{Ti}) : (x_{Sn} - x_{Ti})$ will equal to the Cu:Sn ratio in the Cu-Sn binary compounds.

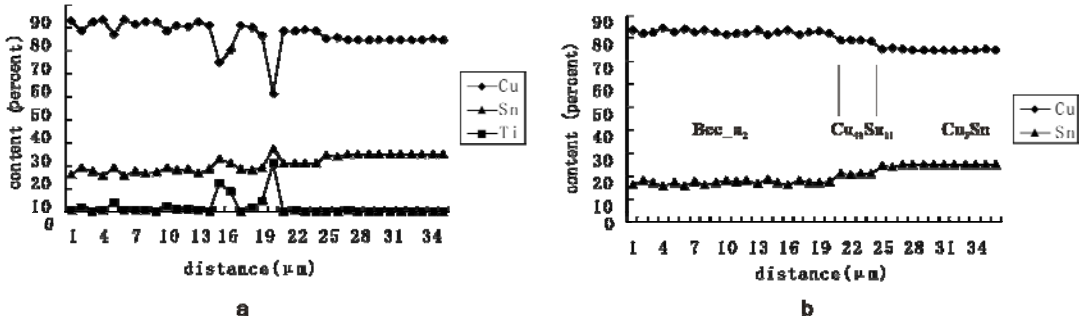

Fig.17 An example for data treatment of CuSnTi and IMCs in Cu-Sn binary system.

(a) original data; (b) calculated results.

Zigzag and disordered raw data of a composition profile measured by EPMA in this work is shown in Fig.4(a) and transferred to Fig.4(b) using new approach where the composition of Cu-Sn binary compounds in equilibrium with CuSnTi is presented. As indicated in Fig.4(b), the Cu:Sn ratio obtained by new approach is regular and consistent with those of the Cu-Sn binary compounds. This means our assumptions are reasonable. Only the Bcc_a_2 composition changes away a little bit, and $x_{(Cu,Bcc\_a_2)}$ is slight higher than that in binary system. The reason is attributed to the Ti solubility change in Bcc_a_2.

3.3.4. Phase Relations and Isothermal Section

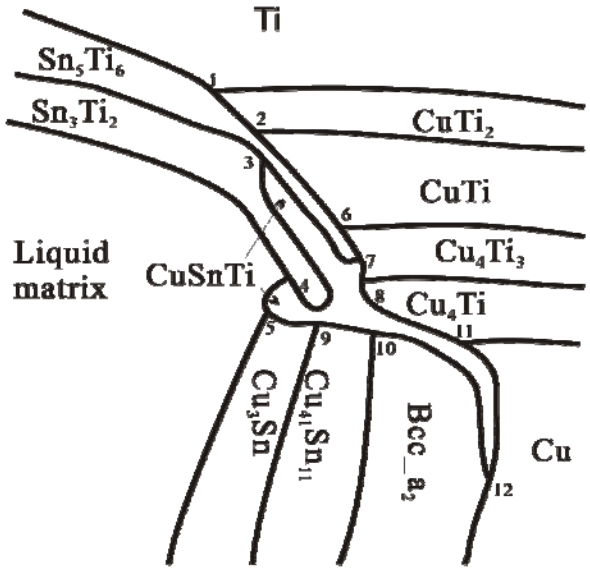

1 $CuTi_2+Sn_5Ti_6+Ti$
2 $CuTi_2+CuTi+Sn_5Ti6$
3 $Sn_5Ti_6+Sn_3Ti_2+CuSnTi$
4 $Liquid+Sn_3Ti_2+CuSnTi$
5 $Liquid+CuSnTi+Cu_3Sn$
6 $CuTi+Cu_4Ti_3+Sn_5Ti_6$
7 $CuSnTi+Cu_4Ti_3+Sn_5Ti_6$
8 $CuSnTi+Cu_4Ti_3+Cu_4Ti$
9 $CuSnTi+Cu_3Sn+Cu_{41}Sn_{11}$
10 $CuSnTi+Cu_{41}Sn_{11}+Bcc\_a_2$
11 $CuSnTi+Cu_4Ti+Cu$
12 $CuSnTi+Bcc\_a_2+Cu$

Fig.18 Schematic diagram of the diffusion-triple of the Cu-Sn-Ti ternary system at 823K.

Based on above discussions, a schematic diagram of phase distribution in Cu-Sn-Ti solid-solid-liquid triple at 823K can be drawn and represented in Fig.18 where a line denotes an interface between two phases and a numbered tri-junction point indicates a three-phase equilibrium. Because the morphology of the well dispersed particles are very complex, they are not illustrated in Fig.18. In addition, this treatment will not influence the phase relationship of the system.

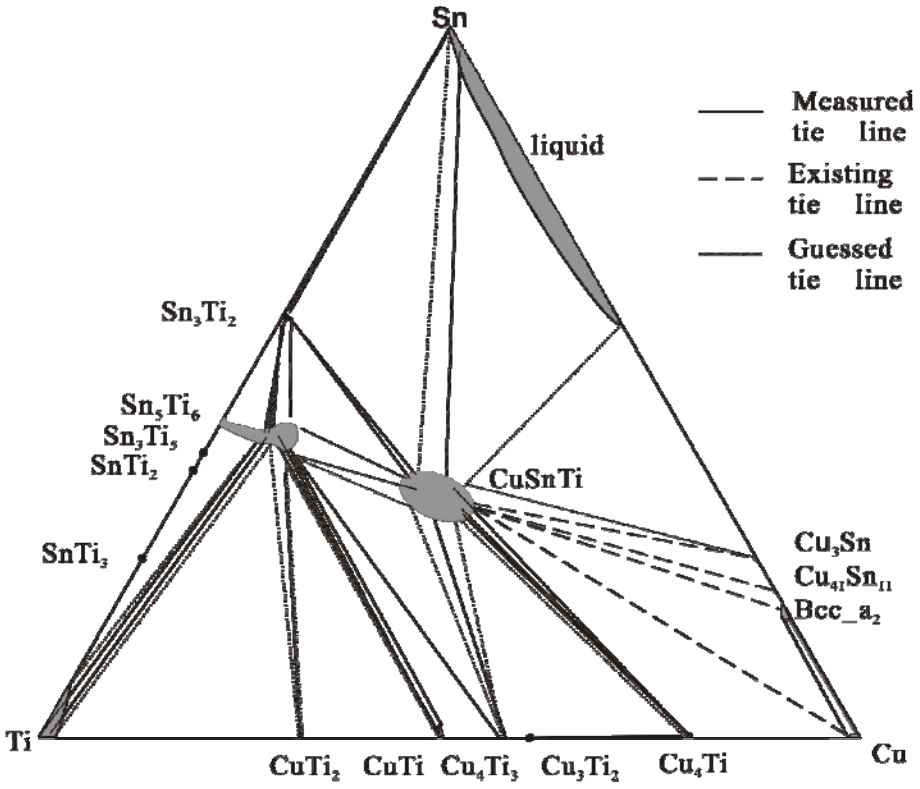

Fig.19 The isothermal section of the Cu-Sn-Ti ternary system at 823K. (The continuous tie-lines are defined from the extrapolation of composition profiles of EPMA by taking advantage of the local equilibrium at interfaces, the dashed-broken lines are tie-lines existing in samples but cannot be measured accurately in this work, and the dashed lines show estimated tie-triangles for 3-phase equilibria).

Note all the three-phase equilibria (1 to 12) are labeled in Fig.18. The EPMA was performed along line perpendicular to interface between each two adjacent phases, and a series of composition profiles are obtained. Subsequently, by extrapolating the composition profiles to the corresponding interfaces in the diffusion-triple, a series of tie-lines are determined and listed in Table 1. Because of the electron scattering effect, it is difficult to measure the composition near the tri-junction points. Thus, the three-phase equilibria are estimated according to the two-phase equilibria. Based on the data listed in Table 1 and combined with Fig.18, an isothermal section of the Cu-Sn-Ti system at 823K is established and illustrated in Fig.19.

It should be noted here that because the stable binary compounds, Sn_5Ti_6, $SnTi_2$, $SnTi_3$, and Cu_3Ti_2 (demonstrated in Fig.19 with little solid black dots) are not observed in this work, the phase equilibria involving these phases in the Ti-rich corner are not determined in the present work. Further investigation in this area is necessary.

3.4. Conclusions

The isothermal section in the Cu-Sn enrich part of the Cu-Sn-Ti ternary system at 823K was determined by using solid-solid-liquid diffusion triple approach. One ternary compound CuSnTi was found, and 12 three-phase fields were detected. The following 10 three-phase regions are well established: $CuTi_2$+CuTi+Sn_5Ti_6, Sn_5Ti_6+Sn_3Ti_2+CuSnTi, Liquid+Sn_3Ti_2+CuSnTi, Liquid+CuSnTi+Cu_3Sn, CuTi+Cu_4Ti_3+Sn_5Ti_6, CuSnTi+Cu_4Ti_3+Sn_5Ti_6, CuSnTi+Cu_3Sn+$Cu_{41}Sn_{11}$, CuSnTi+$Cu_{41}Sn_{11}$+Bcc_a_2, CuSnTi+Cu_4Ti+Cu, and CuSnTi+Bcc_a_2+Cu. Phase relations in the Ti-enrich corner of this system require further investigation.

Table 4 Extrapolated compositions (at. %) of the phases in equilibrium at 823K

Cu- Cu_4Ti			
Cu	Sn	Cu	Sn
96.17	0.09	79.80	0.05
Cu_4Ti_3- Sn_5Ti_6			
Cu	Sn	Cu	Sn
55.80	0.22	10.17	40.69
CuTi- $CuTi_2$			
Cu	Sn	Cu	Sn
47.67	0.05	31.89	0.06
48.39	0.07	33.02	0.06
48.49	0.03	31.63	0.03
CuTi- Cu_4Ti_3			
Cu	Sn	Cu	Sn
49.09	0.09	55.44	0.06
49.12	0.07	55.84	0.10
49.31	0.05	55.67	0.04
49.79	0.07	55.94	0.05
49.91	0.05	55.43	0.04
Cu_4Ti_3- Cu_4Ti			
Cu	Sn	Cu	Sn
57.09	0.06	78.35	0.06
57.28	0.09	78.16	0.14
57.35	0.06	78.10	0.11
CuTi- Sn_5Ti_6			
Cu	Sn	Cu	Sn
47.78	2.03	10.94	39.87
48.65	0.18	8.04	42.33
48.82	0.23	7.92	41.66
$CuTi_2$-Ti			
Cu	Sn	Cu	Sn
30.55	0.09	2.11	0.13
31.13	0.06	2.10	0.11
31.49	0.06	2.08	0.10
Ti- Sn_5Ti_6			
Cu	Sn	Cu	Sn
0.13	0.24	5.65	41.44
0.81	0.36	6.06	42.79
1.08	0.47	6.71	42.29
Sn_3Ti_2- Sn_5Ti_6			
Cu	Sn	Cu	Sn
0.31	59.38	6.09	42.73
0.54	58.07	6.79	43.42
0.68	57.89	6.58	42.68
1.52	58.53	8.04	45.18

Sn_3Ti_2-Sn			
Cu	Sn	Cu	Sn
0.56	59.93	0.29	98.51
Cu-Bcc_a_2			
Cu	Sn	Cu	Sn
98.32	0.19	82.36	16.58
99.36	0.57	82.16	17.75
99.58	0.22	83.11	16.51
99.69	0.30	81.39	18.58
Bcc_a_2-$Cu_{41}Sn_{11}$			
Cu	Sn	Cu	Sn
82.45	17.52	79.51	20.44
83.47	16.22	79.46	20.53
$Cu_{41}Sn_{11}$-Cu_3Sn			
Cu	Sn	Cu	Sn
78.71	21.27	75.07	24.91
78.97	21.03	74.56	25.44
79.23	20.77	75.08	24.90
Cu_4Ti_3-CuSnTi			
Cu	Sn	Cu	Sn
56.54	0.17	31.22	33.82
Sn_3Ti_2-CuSnTi			
Cu	Sn	Cu	Sn
0.75	59.19	27.03	36.41
3.18	57.21	27.53	36.85
Cu_4Ti -CuSnTi			
Cu	Sn	Cu	Sn
78.56	0.53	32.94	35.12
79.32	0.11	35.36	32.04
79.33	0.10	35.89	31.42
Sn-CuSnTi			
Cu	Sn	Cu	Sn
3.03	96.40	31.16	36.75
Sn_5Ti_6-CuSnTi			
Cu	Sn	Cu	Sn
10.22	43.59	26.67	36.48
10.94	39.87	28.79	34.75
$CuTi_2$- Sn_5Ti_6			
Cu	Sn	Cu	Sn
31.30	1.04	11.80	36.86

Chapter 4. Phase evolution when Sn reacting with Cu-Ti compounds at 823K

4.1. Experimental procedure

The experimental procedure is similar with that described in Section 3.2, the difference lays in that Sn was applied as start material.

4.2. morphology variation of (Cu/Ti)/Sn diffusion triple at 823K

The starting morphology of Cu/Ti diffusion couple is the same as shown in **Fig.12**. After annealing at 823K with Sn for various of times, the Cu plate and part of Cu-Ti binary compounds solute into molten Sn, and the morphology are shown in Fig.20~Fig.24.

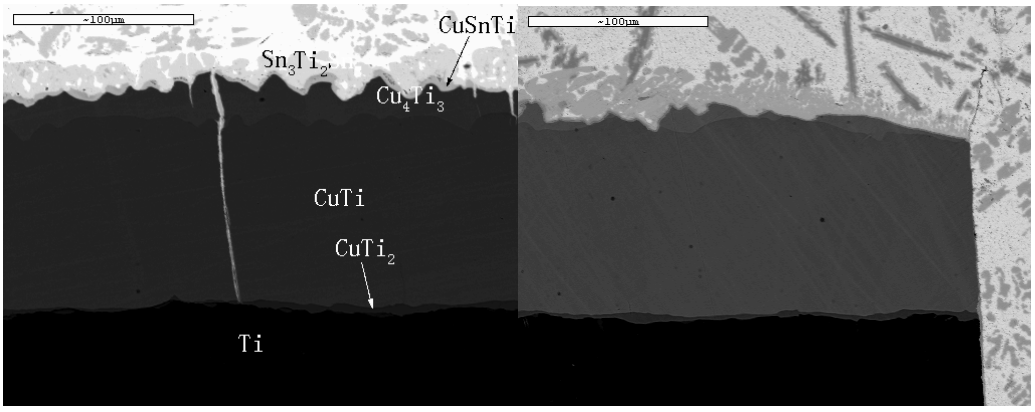

a b

Fig.20 The morphology of Cu-Ti/Sn diffusion triple annealed at 823K for 15 mins.

Fig.20 shows the morphology of samples annealed at 823K for 15 mins,. Cu and Cu_4Ti have dissolved into Sn. Cu_4Ti_3 is also partly dissolved into liquid. In Fig.20(a)，

the white part is Sn, including dendrite Cu_3Sn. From top to bottom, the continuous layers were Ti2Sn3, CuSnTi, Cu_4Ti_3, CuTi, $CuTi_2$ and Ti respectively. It should be noticed that in Fig.20(a), Sn_3Ti_2 is not continuous. Between Sn_3Ti_2 blocks, it is liquid piercing through and contact with CuSnTi, results in three-phase region liquid+CuSnTi+Sn_3Ti_2. In Fig.20(b), similar morphology as that in Fig.20(a) is found.

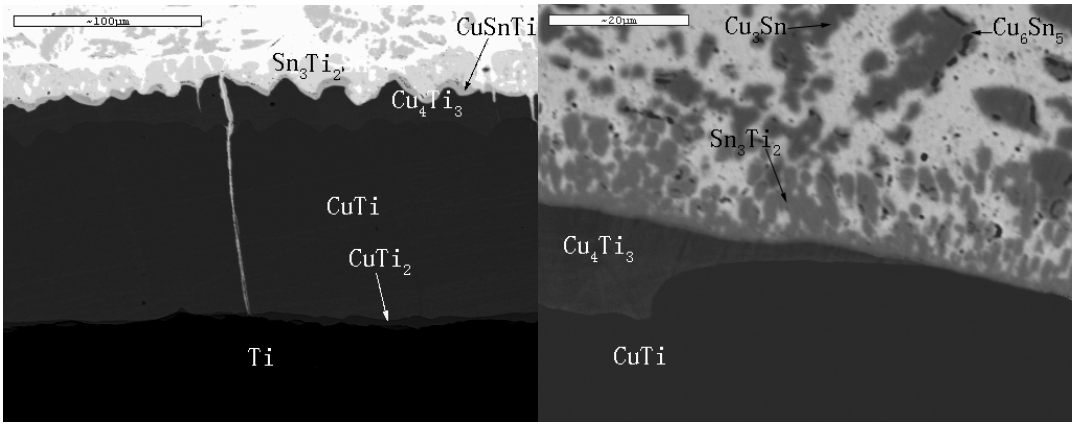

Fig.21 The morphology of Cu-Ti/Sn diffusion triple annealed at 823K for 30 mins.

Fig.21 shows the morphology of samples annealed at 823K for 30 mins. The phases appear in Fig.21(a) and their space sequence is the same as that in Fig.20(a). Only for Sn_3Ti_2 growing thicker with time prolonging, and connected to form a continuous layer, separating Cu_4Ti_3 and liquid away from each other. Meanwhile, at the side part (Fig.21(b)), the morphology changed little during the period from 15 to 30 mins. The surface of Cu-Ti binary compounds has changed into a slope.

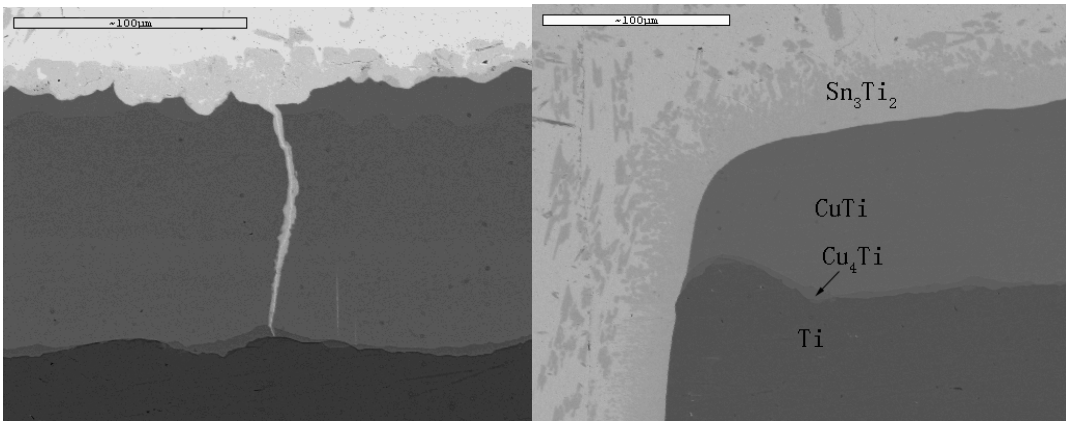

Fig.22 the morphology of sample annealed at 823K for 120 mins.

Fig.22 shows the morphology of sample annealed at 823K for 120 mins. Cu_4Ti_3 was thinner compared with in Fig.20 The most significantly difference in Fig.5 is the

thin layer phase above Cu_4Ti_3, whose composition is about Cu6Sn47Ti47, not CuSnTi as shown in Fig.20. Compared with S. Hamar-Thibault's work, that the ternary phase Ti_5Sn_3Cu with amounts of 52at.% of Ti, 33 at.% of Sn and 11~13 at.% of Cu, only stable above 700℃and according to other data gotten from this work, this layer was assumed to be Sn_5Ti_6 with a certain amount Cu dissolution. Compared with shown in Fig.20(a), the CuSnTi and Cu_4Ti_3 between Ti2Sn3 and CuTi are disappeared partly in Fig.22(a). Cu_4Ti_3 was still a continuous layer, but CuSnTi next to it was not continuous any longer. Sn_5Ti_6 takes place of CuSnTi at some places. The reason for phase changing should be though Cu_4Ti_3 is considered stoichiometric composition, it actually has a little composition range. Naturally, Ti content in Cu_4Ti_3 at the Ti matrix side is higher than that at the Cu matrix side; Cu content is in the reverse. There is a critical point for Ti content in Cu_4Ti_3 that the tie-lines with one end at Cu_4Ti_3 switch the other end from CuSnTi to Ti6Sn5. This agrees well with the isothermal section obtained in Chapter 3.

Reactions between 30 and 120 mins should be: 1. Sn_5Ti_6 nucleated 2. part of CuSnTi disappeared.

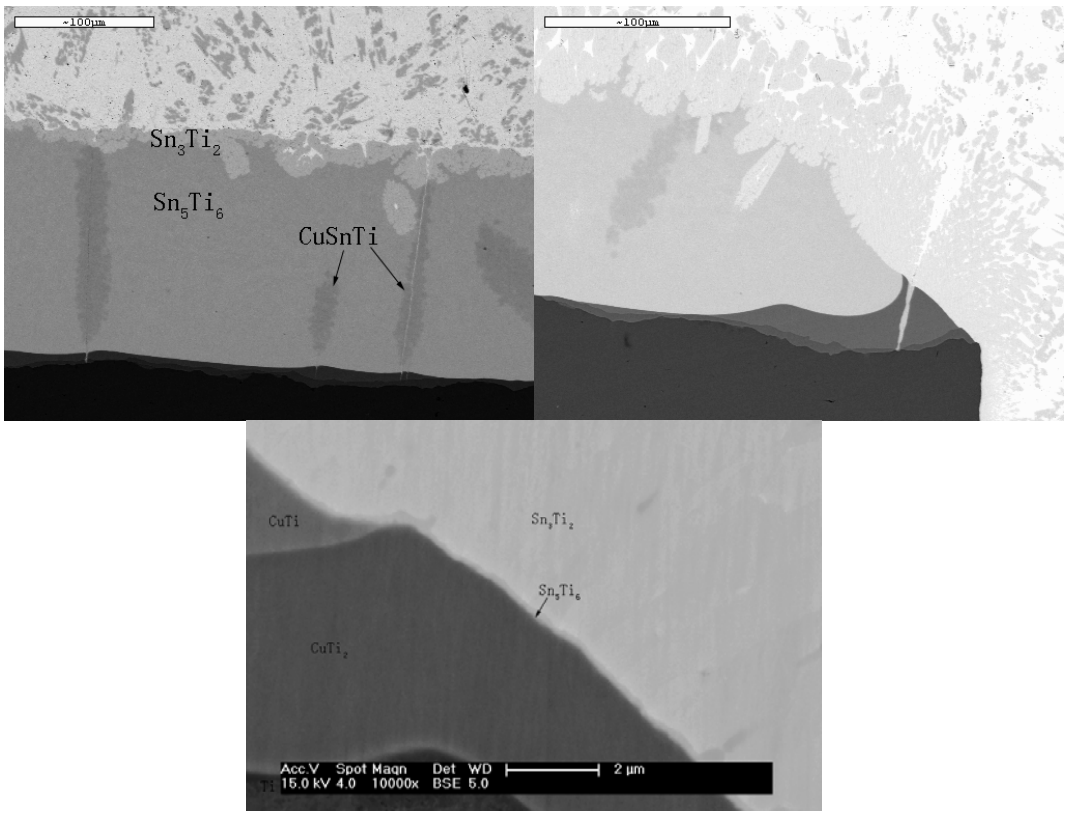

Fig.23 the morphology of sample annealed at 823K for 180 mins.

Fig.23 shows the morphology of sample annealed at 823K for 180 mins. After

annealing for 180 mins, most of CuTi dissolves and Ti6Sn5 with amounts of nearly 48 at.% of Ti, 43 at.% of Sn and 8-10 at.% of Cu appears. Ternary phase CuSnTi with composition about Cu30Sn35Ti35 in leaf-shape can be seen inside Ti6Sn5.

Fig.23(b) is SEM photo of the right part of this sample. There was still some CuTi remaining here. The right side of CuTi was a straight slope caused by solution of CuTi into Sn. Meanwhile, the left side shows a curve like a quarter of circle. The shape should be caused by diffusion of Cu and Sn through Sn_5Ti_6. Comparing different curves of both sides, we can concluded existence of Sn_5Ti_6 can accelerate consuming of CuTi.

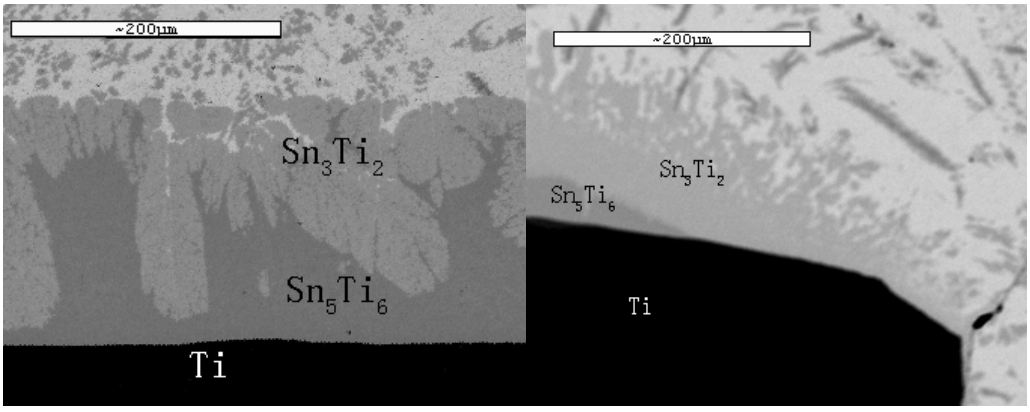

a b

Fig.24 the morphology of Cu-Ti/Sn diffusion triple annealed at 823K for 480 mins.

Fig.24 shows the morphology of Cu-Ti/Sn diffusion triple annealed at 823K for 480 mins. After annealing for 480 mins, CuTi , $CuTi_2$, and CuSnTi disappear. Meanwhile, Ti6Sn5 partly dissolve, and Ti2Sn3 forms. Due to infinite supplement of Sn, tendency should be Ti6Sn5 would change to Sn_3Ti_2, which can be seen in Fig.24(b), where Ti6Sn5 has become so thin that can not be seen in this picture.

4.3. Disscussions

Comparing Fig.20~Fig.24, some interesting phenomena can be fond.

4.3.1. Different consume speed among different Cu-Ti compounds

Though velocity of Cu solute into molten is large, it is greatly enhanced by

addition of titanium. In less than 15 mins, Cu plate (thicker than 3mm) and Cu_4Ti disappeared, leaving Cu_4Ti_3 directly contacted with liquid Sn (Fig.20). The reason is not clear.

It is believed that at the initial stage of solid-liquid reacting, solid matrix dissolve into liquid and form a thin layer of saturated solution, and then IMCs formed. But for this system, both Cu and Cu_4Ti disappear in less than 15 mins(Fig.20), indicate that both dissolve and diffusion of Cu in liquid Sn is rapid. After 15 mins, there are two phases, Sn_3Ti_2 and CuSnTi formed between liquid and remaining Cu-Ti IMCs. Sn_3Ti_2 indicates that liquid Sn around it has reached saturation. Due to negligible solubility of Ti in Sn, even saturated Ti-Sn solution can be considered as diluent. In this situation, diffusion flux can be very small because of little concentration grade. Thus, enough Ti can be entrapped in Sn_3Ti_2. At the corner of this sample (Fig.20 b), Sn_3Ti_2 is much thinner, this can be applied as an evidence of former analyses. CuSnTi can be found in this sample. Only at the central part (Fig.20 a), in Fig.20 b, no formed CuSnTi was found. This should caused by lower Ti concentration and weaker protection provided by thinner Sn_3Ti_2.

Comparing Fig.21 and Fig.20, their morphology is similar to each other. The thickness of Sn_3Ti_2, CuSnTi, and Cu_4Ti_3 changes little. Even at the corner, similar shape was remaining. It is interesting that there are two depressed hole locate at their corner. They look like each other so much that the author was confused if the photos were taken from the same sample. Similar morphology indicates that reaction speed was rather slow during this period (from 15 mins to 30 mins).

After annealing for 120 mins, the morphology and phases appeared in the diffusion couples has changed a little. Obviously, consuming of Cu_4Ti_3 is slow. Contrary to Cu and Cu_4Ti, both of which is thicker than Cu_4Ti_3, but disappeared in less than 15 mins, it takes more than 2 hours for exhausting a thin layer (about 10 micrometers) of Cu_4Ti_3.

According to Fig.23, CuTi (about 100 micrometers) almost consumed in 60 mins. While total thickness of remaining Cu-Ti compounds and compounds formed during annealing maintains almost the same. Variation in this period requires diffusions in two opposite directions. The first is Cu dissolve into Sn through Sn_5Ti_6 and Sn_3Ti_2; the other is Sn diffusion from liquid matrix to Cu-Ti compounds by the opposite opposition. Comparing changing speed between Cu_4Ti_3 and CuTi, great difference can be found.

As shown in Fig.24, after annealing for 480 mins, CuTi , $CuTi_2$, and CuSnTi

disappear. Meanwhile, Ti6Sn5 partly dissolve, and Ti2Sn3 forms. Due to infinite supplement of Sn, tendency should be Ti6Sn5 would change to Ti2Sn3, which can be seen in Fig.24(b), where Ti6Sn5 has disappeared.

The consume speed of compounds in this work is surmised in Table 5:

Table 5 consume speed of different compounds

Phase	Speed	Consumetime	Referencepicture
Cu	fast	Lessthan15minutes	Fig.20
Cu_4Ti	fast	Lessthan15minutes	Fig.20
Cu_4Ti_3	slow	2hours	Fig.20&Fig.22
CuTi	medim	1hour	Fig.22&Fig.23
$CuTi_2$	unknown		
Sn_3Ti_2	unconsumed		
Sn_5Ti_6	slow	Morethan5hours	Fig.23&Fig.24

4.3.2. Column grains and anisotropism

Great anisotropism exists in Cu-Ti diffusion layer. This can be concluded by several phenomenal.

The most obvious phenomenal is different speed in different direction. From Fig.20~Fig.24, it can be found that almost all reactions are progressing vertically to initial Cu-Ti interface. CuTi binary phase is the most typical example. It takes about 120 mins to consume Cu, Cu_4Ti and Cu_4Ti_3 which initially protect CuTi to contact with Liquid. But after they were exhausted, there is two layers of Sn-Ti compounds. Sn_3Ti_2 contact with liquid matrix, and a thin layer type Sn_5Ti_6 formed when Cu_4Ti_3 was nearly exhausted. Subsequently the reaction speed is enhanced greatly. In next 60 mins, about 90 percents of CuTi conversed into Sn_5Ti_6 from interface where was adjacent to Cu_4Ti_3 at the beginning and grows to one direction. Comparatively, at the interface where initially contact with molten Sn, reaction rate is much lower. Until after annealing for 180 mins, the angle between Cu-Ti compounds and Ti is still about 45º, and distance from Ti to CuTi compounds is very little (only several micrometers). Great difference exists between diffusion rates in two vertical directions.

The other phenomenal lays in that quick diffusion path that found in every sample made from Cu-Ti diffusion couple and molten Sn. We name these quick diffusion path white line because of they are white in BSE images and in the shape of "line". As

shown in Fig.20, in less than 15 mins, a white line has formed vertically to Cu-Ti interface and get through all Cu-Ti compounds. Obviously white line is quick diffusion path. The cause of quickly diffusion path is considered to be defects such as cracks, grain boundary etc. [1] As shown in **Fig.12**, Cu-Ti diffusion couple were well welded and Cu-Ti IMCs were formed during annealing at 1023K, no defect was found initially. Therefore, there must be a phase boundary located at the place where white line lays at. Since the phase boundaries are parallel with IMCs' growth direction, the Cu-Ti compounds should be column grains with certain orientation of crystal.

4.3.3. Changing tri-junction

In diffusion couple approach, phase boundary takes critical importance. Because of limitation of freedom degree, phase boundaries in binary system must keep plane and continuous. However, for diffusion couple contains three components, one additional freedom is available, phase boundary do not necessary to be plane or continuous, dispersed particles are also with possibility. Waviness of phase boundary or dispersed particles induces two-phase regions; discontinuous phase boundary result in geometrical tri-junctions in diffusion couples and three phase fields in isothermal sections. The scheme is shown below:

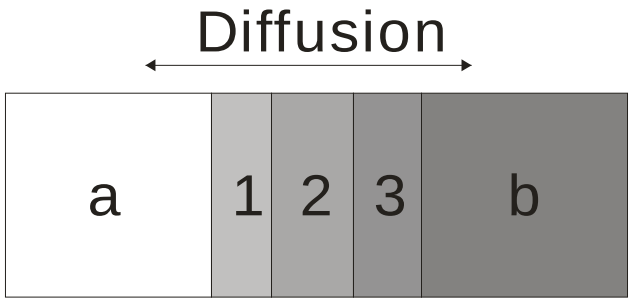

Fig. 25 scheme of diffusion couple with two elements and three compounds.

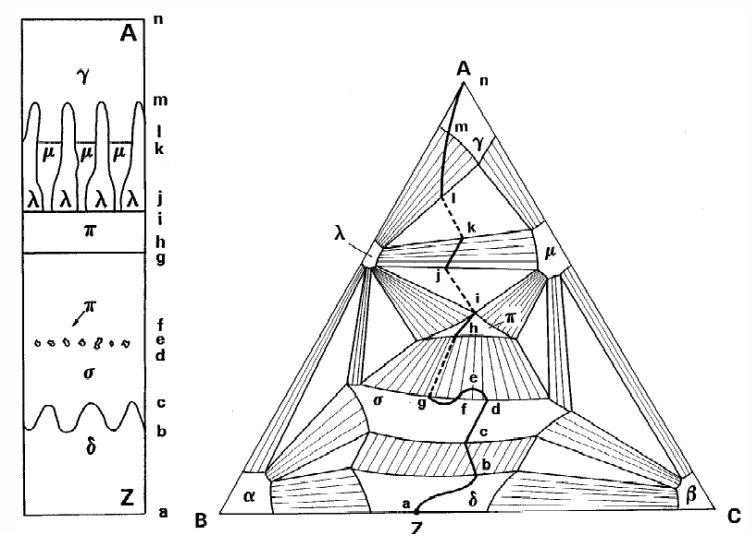

Fig.26 scheme of diffusion couple with three components.

As shown in Fig. 25 and Fig.26, tri-junctions are the most significant difference between diffusion couples made of two and three components. Therefore all tri-junctions appeared in this work should be checked out.

Combining Fig.20~Fig.24, all appeared tri-junctions are listed in Table 6, in which tri-junctions are given in the form of three-phase equilibria. Three-phase equilibria caused by the formation of white line are not listed because there are tinny structures too complex to be discussed here and white lines are too different from other parts.

Table 6 tri-junctions detected in this work

annealing time (min)	three-phase equlibrium
15	CuSnTi+Sn3Ti2+liquid
30	none
120	Sn3Ti2+Sn5Ti6+CuSnTi Sn5Ti6+CuSnTi+Cu4Ti3 Sn5Ti6+Cu4Ti3+CuTi
180	Sn3Ti2+Sn5Ti6+CuSnTi Sn3Ti2+CuSnTi+Sn Sn5Ti6+CuTi+CuTi2 Sn5Ti6+CuTi2+Ti
480	none

4.3.4. Different space sequence and diffusion paths

Diffusion paths can be applied to illustrate morphology of diffusion couples. Diffusion paths can prove guidelines for understanding phase formation sequence, evaluating activity variation with changing of compositions. Moreover, analyses of diffusion paths with composition, time etc. can help understanding relationships between different elements.

In this work, initially (after annealing at 1023K) material is not pure metal or homogeneous alloy. There are six layers, Cu, Cu_4Ti, Cu_4Ti_3, CuTi, $CuTi_2$ and Ti in Cu-Ti diffusion couple. Fortunately, because of anisotropism of Cu-Ti binary compounds, phase evolution are processing in one direction， this make it possible to determine several diffusion paths starting at different Cu-Ti binary compounds and compare them in a series of similar samples among which only annealing time varies. Due to fast solution of Cu and Cu_4Ti into molten Sn, diffusion path about them are not detected.

After 15 mins, the phase structure from Cu_4Ti_3 is, as illustrated in Fig.27(a). The phase structure is Cu_4Ti_3/CuSnTi//Sn_3Ti_2+liquid/liquid. The diffusion path firstly crosses the two-phase equilibrium region of Cu_4Ti_3+CuSnTi Since the interface between Cu_4Ti_3 and CuSnTi is not planar, the diffusion path is not parallel to one tie-line. In Sn-Ti binary phase diagram, Sn_3Ti_2 forms from a peritectic reaction, according to the size of Sn_3Ti_2, it must forms during annealing process. So after crossing single-phase region of CuSnTi, because both of the later two phases contact with CuSnTi, the diffusion path reaches three-phase region CuSnTi+Sn_3Ti_2+liquid. Finally, the diffusion path crosses two-phase equilibrium of Sn_3Ti_2+liquid.

The phase structure after annealing for 30 mins is Cu_4Ti_3/CuSnTi/Sn_3Ti_2/Sn_3Ti_2+ liquid/liquid, as illustrated in Fig.27(b). The diffusion path is similar as that in Fig.27(a). But after 30 mins, Sn_3Ti_2 blocks existing between CuSnTi and liquid has connected with each other, formed continuous layer. So the diffusion path get through two-phase equilibria CuSnTi+Sn_3Ti_2. Lastly, diffusion path cross two-phase equilibrium of Sn_3Ti_2+liquid.

Fig.27(c) shows diffusion path that illustrate the phase structure after annealing for 120 mins. The phase structure is CuTi/CuTi+Cu_4Ti_3+Sn_5Ti_6/Cu_4Ti_3+Sn_5Ti_6/Cu_4Ti_3+ Sn_5Ti_6+CuSnTi/Sn_5Ti_6+CuSnTi/Sn_5Ti_6+CuSnTi+Sn_3Ti_2/Sn_3Ti_2/Sn_3Ti_2+liquid/liquid

After annealing for 120 mins, due to consuming of Cu_4Ti_3, it is no longer continuous. CuTi contact with Sn_5Ti_6 where Cu_4Ti_3 breaks, thus three-phase equilibrium CuTi+Cu_4Ti_3+Sn_5Ti_6 forms. Therefore, the diffusion path start at Cu_4Ti_3 and firstly get through the mentioned three-phase region. Because in no circumstance can CuTi be contact with CuSnTi, there must be a layer, no mater how thin is it, is formed by two phases, Cu_4Ti_3 and Sn_5Ti_6, so a fragment of diffusion path locates at two-phase region of Cu_4Ti_3 and Sn_5Ti_6. The diffusion path does not reach single-phase region of Sn_5Ti_6 because it is not a continuous layer. Cu_4Ti_3 is covered by Sn_5Ti_6 and CuSnTi completely, this lead the diffusion path get cross three-phase region Cu_4Ti_3+Sn_5Ti_6+CuSnTi and reach two-phase equilibrium Sn_5Ti_6+CuSnTi. The phase locates at the other side of the layer formed by CuSnTi and Sn_5Ti_6 is Sn_3Ti_2, which also connect with liquid. There for the diffusion path get through three-phase region CuSnTi+Sn_5Ti_6+Sn_3Ti_2, pass single phase region of Sn_3Ti_2, get through two phase field of Sn_3Ti_2+liquid, and finally ends at liquid phase.

The phase structure after annealing for 180 mins is $CuTi_2$/$CuTi_2$+CuTi+Sn_5Ti_6/ $CuTi_2$+Sn_5Ti_6/Sn_5Ti_6/Sn_5Ti_6+CuSnTi/Sn_5Ti_6+CuSnTi+Sn_3Ti_2/Sn_3Ti_2/Sn_3Ti_2+liquid/ liquid, as illustrated in Fig.27(d). After annealing for 180 mins, the formed thickest Cu-Ti binary compound CuTi is almost exhausted and becomes discontinuous. Three-phase equilibrium $CuTi_2$+CuTi+Sn_5Ti_6 forms and diffusion path crosses corresponding three-phase region. CuTi and Sn_5Ti_6 form a two-phase region followed by Sn_5Ti_6 single-phase layer. It cannot be neglected that there are many leaf-shape CuSnTi phase blocks in Sn_5Ti_6 layer. So the diffusion path crossed Sn_5Ti_6 enters two-phase region Sn_5Ti_6+CuSnTi. Both Sn_5Ti_6 and CuSnTi are contacting with Sn_3Ti_2, so the diffusion path crosses three-phase region Sn_5Ti_6+CuSnTi+Sn_3Ti_2. Finally the diffusion path get through two-phase region Sn_3Ti_2+liquid and ends at liquid matrix.

The phase structure after annealing for 480 mins is Ti/Ti6Sn5/Ti6Sn5+Sn_3Ti_2/ Sn_3Ti_2, as illustrated in Fig.27(e). All Cu-Ti binary compounds have disappeared and replaced by Sn_5Ti_6 and Sn_3Ti_2. The diffusion path starts at Ti, cross two-phase equilibrium Ti+Sn_5Ti_6. Because interface between Ti and Sn_5Ti_6 is planner, the diffusion path is parallel with one of their tie-lines. After cross single-phase region of Sn_5Ti_6, the diffusion path get cross two-phase region of Sn_5Ti_6 and Sn_3Ti_2. Because their phase boundary is not planner, the diffusion path crosses with their tie-lines. Subsequently, the diffusion path get through single phase region of Sn_3Ti_2, two-phase region of Sn_3Ti_2 and liquid and ends at liquid phase region.

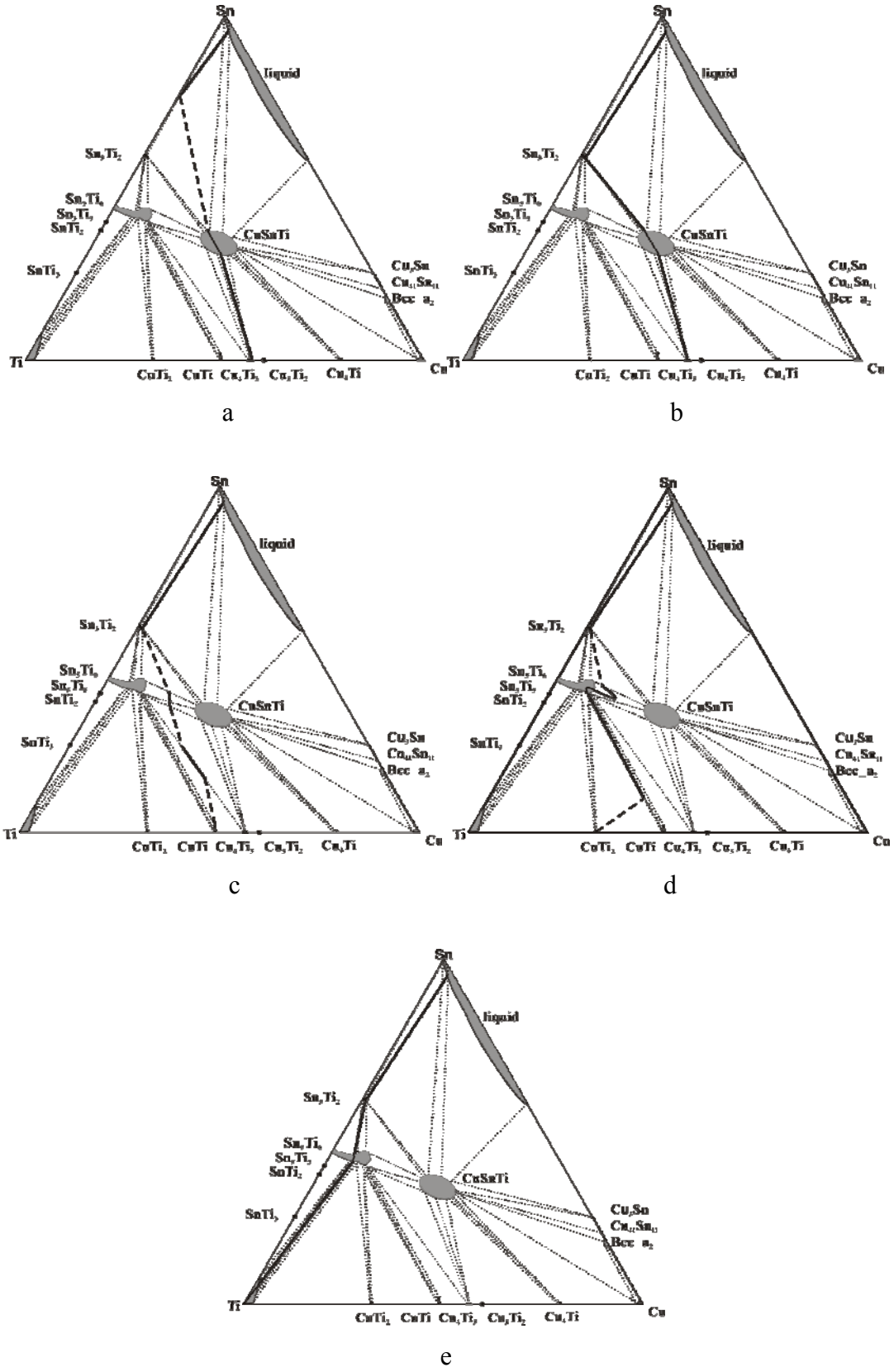

Fig.27 the diffusion paths in the (Cu/Ti)/Sn diffusion couple.

(a) 15 mins; (b) 30 mins; (c) 120 mins; (d) 180 mins; (e) 480 mins

Comparing Fig.27(a)~Fig.27(e), it is clearly that with increasing of time, the diffusion path moves to Sn-Ti side in the isothermal section. That is because the directional reactions appearing in this experiment. Cu-Ti binary compounds transport into Sn-Ti binary compounds, Sn_3Ti_2 and Sn_5Ti_6, one by one, from Cu side to Ti side.

CuSnTi ternary phase appears in the annealing process. As indicated in Fig.20, CuSnTi appears in less than 15 mins, and enter the three-phase equilibrium CuSnTi+ Sn_3Ti_2+liquid three-phase equilibrium. In Fig.20 and Fig.21, CuSnTi is continuous and in equilibrium with Cu_4Ti_3. But after annealing for 120 mins, as shown in Fig.22, CuSnTi is no longer continuous, Sn_5Ti_6 forms and three-phase equilibrium Cu_4Ti_3+ CuSnTi+Sn_5Ti_6 forms. That indicates both CuSnTi and Sn_5Ti_6 can form between Cu_4Ti_3 and Sn_3Ti_2. Which of them forms should be determined the composition of Cu_4Ti_3 and Sn_3Ti_2 besides the interface. Since Sn_3Ti_2 forms in the annealing process and contacts with liquid, the composition change must be little. Therefore, composition change of Cu_4Ti_3 should be the reason. Though composition range of Cu_4Ti_3 is very narrow, there must be an composition grade in it, that is at near the Cu side, Cu content is higher, and Ti content is higher in the other side. In the annealing process, Cu_4Ti_3 consumes with increasing of time and becomes thinner, interface moving from Cu side to Ti side, Cu concentration decreases and Ti concentration increases. In the isothermal section we can conclude with Ti concentration increasing, the phase in equilibrium indeed changes from CuSnTi To Sn_5Ti_6. As indicated in isothermal section, CuSnTi is not in equilibrium with CuTi, $CuTi_2$ or Ti. And in this work CuSnTi layer between Cu_4Ti_3 and Sn_3Ti_2 disappears after CuTi is exhausted. The isothermal section and the phenomenal aggress well with each other.

It should be noticed that there is an interesting phenomenal in the sample annealed for 180 mins that the CuSnTi phase forms around quick diffusion path of liquid and grows into Sn_5Ti_6. Therefore, Sn_5Ti_6 and CuSnTi are in equilibrium with each other, and CuSnTi contact liquid phase in the quick diffusion paths. However, at the vertical direction that also is the direction we drawing diffusion paths, Sn_5Ti_6, as well as CuSnTi, contacts with Sn_3Ti_2, which contact with liquid matrix. Then different phase sequences in two directions are obtained. They are Sn_5Ti_6->CuSnTi->liquid in horizon direction and Sn_5Ti_6->Sn_3Ti_2->liquid in vertical direction (in the image Fig.23(a)). The reason for these two phase sequences is attributed to the difference between the liquid state. The liquid next to Sn_3Ti_2 is opening to the entire liquid matrix, due to very fast diffusion speed in liquid phase, many literatures treat liquid as homogeneous region. Because of

comparatively large quantity of Sn, the liquid matrix can be treated approximately as pure Sn. However, in the quick diffusion path, where Sn quantity is small, treating liquid as pure Sn may deviation from truth too far. Oppositely, because of little amount of liquid phase and the long diffusion distance for Cu and Ti require to escape to liquid matrix, treat the liquid in quick diffusion path as saturate solution is more acceptable. As shown in the isothermal section, both Sn_3Ti_2 and CuSnTi are in equilibrium with liquid phase. There must be a composition point at the edge of liquid phase region where liquid in equilibrium with Sn_3Ti_2 and CuSnTi. According to the isothermal section, the liquid with more Sn is in equilibrium with Sn_3Ti_2, and the liquid with more Cu content is in equilibrium with CuSnTi. That is the reason of formation of two different space sequences.

4.4. Conclusions

With addition of Ti, the consumption speed of Cu is greatly enhanced. At 823K, Cu plate with thickness of about 3mm solute into Sn in less than 15 mins. Cu-Ti binary compounds still have different consumption speed in molten Sn.

The grown out Cu-Ti binary compounds show great anisotropism in this work, and there are quick diffusion paths vertical to Cu-Ti interface form in them.

With progressing of annealing, different tri-junctions which mean correlative three-phase regions in the isothermal section appear in the samples sequently at 823K

After annealed at 823K for different times from 15 mins to 480 mins, the morphologies of diffusion zones are illustrated with diffusion paths.

Chapter 5. Conclusions and Prospect

5.1. Conclusions

The Ti/Sn and Cu/Sn solid/liquid diffusion couples and the Cu/Ti diffusion couples are made and examined. Only Sn_3Ti_2 forms if Ti/Sn solid/liquid diffusion couples are annealed at 873K for 30~160 mins. When annealed at 808K for 10 mins, only Cu_3Sn forms in Cu/Sn solid/liquid diffusion couple. With the annealed time increasing, $Cu_{41}Sn_{11}$ layer forms between Cu and Cu_3Sn in 30 min, and then bcc-a_2 layer forms between Cu and $Cu_{41}Sn_{11}$ in 60 min. After annealing at 1023K for 1000 hours, four compounds, $CuTi_2$, CuTi, Cu_4Ti_3 and Cu_4Ti form in Cu/Ti diffusion couple while Cu_3Ti_2 is absent. The interfacial reaction process and phase formation sequence has been successfully predicted with the maximum driving force model using the Thermo-Calc software.

Phase relations in the Sn-Cu side of the Cu-Sn-Ti system at 823K were determined by diffusion-triple approach along with Electron Probe Microanalysis (EPMA) technique. A ternary phase, CuSnTi, was detected to have a certain homogeneity range. Except in the Ti-rich corner, phase equilibria in most part of the isothermal section of Cu-Sn-Ti ternary system at 823K were well established. In this isothermal section, 12 three-phase equilibria were proposed, of which 2 three-phase equilibria, $CuTi_2$+Sn_5Ti_6+Ti and CuSnTi+Cu_4Ti_3+Cu_4Ti need further study.

The obtained Cu/Ti diffusion couples were annealing with pure Sn at 823K. with addition of Ti, Cu and Cu_4Ti was exhausted in 15 mins, the other Cu-Ti binary compounds have various of consuming speed. In the annealing process, the Cu-Ti binary compounds show great anisotropism in this work, and there are quick diffusion paths vertical to Cu-Ti interface form in them. With progressing of annealing, different tri-junctions which mean correlative three-phase regions in the isothermal section appear in the samples sequently at 823K. After annealed at 823K for different times from 15 mins to 480 mins, the morphologies of diffusion zones are illustrated with diffusion paths.

5.2. Prospect

Though the isothermal section of Cu-Sn-Ti ternary system at 823K were well established, Sn_5Ti_6, $SnTi_2$, $SnTi_3$, and Cu_3Ti_2 was not detected in this work. The absence of these binary phases means the obtained isothermal section may contain some metastable tie-lines and need future investigation.

The extremely complex morphology of obtained samples bring uncertainty as well as difficulty of analysis into this work, alloy samples may be necessary to confirm the obtained equilibrium.

In order to fully understand the progress of microstructure evolution, investigation of this system at different temperatures is required.

The utilization of Cu-Sn-Ti system is associated with ceramic, diamond, sapphire, and so on. The forth element should be add to this system and examined the influence.

Reference

[1] A.A. Kodentsov, G.F. Bastin, F.J.J. van Loo, The diffusion couple technique in phase diagram determination, J Alloys Compd, 320 (2001) 207–217

[2] F. J. J. van Loo, Multiphase diffusion in binary and ternary solid-state systems, Prog. Solid State Chem. 1990, 20(1), 47-49.

[3] M. Hasebe, T. Nishizawa, in Applications of Phase Diagrams in Metallurgy and Ceramics (Ed: G. C. Carter), NBS Special Publ. #496, Vol. 2 1978, p. 911.

[4] Z. Jin, A study of the range of stability of σ phase in some ternary systems, Scand. J. Metall. 1981, 10(6), 279-287.

[5] J.-C. Zhao, Z. Jin, Determination of phase equilibria in the Ti-Fe-Co system at 900°C, Z. Metallkd. 1990, 81(4), 247-250.

[6] J.-C. Zhao, Z. Jin, P. Huang, Diffusion quadruples for the determination of quaternary phase diagrams applied to FeCoNiCr system, Scr. Metall. 1988, 22(12), 1825-1829.

[7] J.S. Kirkaldy, L.C. Brown, Can. Metall. Quat., 1963, 2, 89.

[8] J.B. Clark, Trans. Met. Soc. AIME, 1963, 227, 1250.

[9] P. Maugis, W.D. Hoffe, J.E. Morral, et al, Multiple interface velocity solutions for ternary biphase infinite diffusion couples, Acta Mater., 1997, 45, 1941-1954.

[10] H. Chen, J.E. Morral, Variation of the effective diffusivity in two-phase regions Acta Mater., 1999, 47, 1175-1180.

[11] T. Helander, J. Ågren, Phenomenological treatment of diffusion in Al-Fe and Al-Ni alloys having B2-B.C.C. ordered structure, Acta Mater., 1999, 47, 1141-1152.

[12] W. Lengauer, Titanium-nitrogen system. A study of phase reactions in the subnitride region by means of diffusion couples, Acta Mater., 1991, 39, 2985-2996.

[13] W. Lengauer, The temperature gradient diffusion couple technique: an application of solid-solid phase reactions for phase diagram imaging, J. Solid State Chem., 1991, 91, 279-285.

[14] J.I. Goldstein, D.E. Newbury, P. Echlin, D.C. Joy, A.D. Romig Jr., C.E. Lyman, C. Fiori, E. Lifshin, Scanning Electron Microscopy and X-ray Microanalysis, Plenum Press, New York, 1992

[15] A.D. Romig Jr., J.I. Goldstein, Determination of the Fe-rich portion of the Fe-Ni-C phase diagram, Metall. Trans. 1978, 9A (11), 1599-1609.

[16] F.J.J. van Loo, J.W.G.A. Vrolijk, G.F. Bastin, phase relations and diffusion paths in the Ti-Ni-Fe system at 900 degree C, J. Less-Common Metals, 1981, 77, 121-130.

[17] F.J.J. van Loo, G.F. Bastin, phase relations and diffusion paths in the Ti-Ni-Co system at 900 degree C, J. Less-Common Metals, 1981, 81, 61-69.

[18] J.A. van Beek, A.A. Kodentsov, F.J.J. van Loo, Phase equilibria in the Ni-Cr-Ti system at 850 °C, J. Alloys Comp., 1998, 270, 218-223.

[19] J.-C. Zhao, M.R. Jackson, L.A. Peluso, Determination of the Nb–Cr–Si phase diagram using diffusion multiples, Acta Mater., 2003, 51, 6395–6405.

[20] J.-C. Zhao, Xuan Zheng, and David G. Cahill, High-throughput diffusion multiples, materialstoday October 2005, 28-37.

[21] J.-C. Zhao, A combinatorial approach for structural materials, Adv. Eng. Mater., 2001, 3 (3), 143-147.

[22] J.-C. Zhao, Combinatorial approaches as effective tools in the study of phase diagrams and composition-structure-property relationships, Progress in Materials Science, v 51, n 5, July, 2006, p 557-631.

[23] T-W Kim, H.-S. Chang, S.-W. Park, Brazing Parameters and Mechanical Properties of Silicon Nitride/Stainless steel joint, Ceramic Engineering and Science

Proceedings, 2001; 22, 4: 627-634.

[24] T.H. Chuang; M.S. Yeh; Y.H. Chai, Brazing of zirconia with AgCuTi and SnAgTi active filler, Metallurgical and Materials Transactions; Jun 2000; 31A, 6; 1591-1597.

[25] O.M. Akselsen, Advances in brazing of ceramics, J. Mater. Sci., 1992, 27: 1989-2000.

[26] J-G Li, Wetting and interfacial bonding of metals with ioncovalent oxides. J Am Ceram Soc 1992;75:3118–26.

[27] XB Zhou, De Hosson JThM. Reactive wetting of liquid metals on ceramic substrates. Acta Mater, 1996;44:421–426.

[28]H. Mizuhara, E. Huebel, Joining ceramic to metal with ductile active filler metal, Weld. J., 1986, 65 (10): 43-45.

[29] T. Yano, H. Suematsu, T. Iseki, High-resolution electron microscopy of a SiC/SiC joint brazed by a Ag-Cu-Ti alloy, J. Mater. Sci. 1988, 23: 3362-3366.

[30] J.K. Boadi, Ti. Yano, T. Iseki, Brazing of pressureless-sintered SiC using Ag-Cu-Ti alloy, Mater. Sci., 1987, 22: 2431-2434.

[31]R. Xu, J.E. Indacochea, Reaction layer characterization of the braze joint of silicon nitride to stainless steel, J. Mater. Eng. Perf., 1994, 3 (5): 596-605.

[32] R.R. Kapoor, T.W. Eagar, Oxidation behavior of silver- and copper-based brazing filler metals for silicon nitride/metal joints, J. Am. Ceram. Soc., 1989, 72 (3): 448-454.

[33] Y.S. Chung, T. Iseki, Interfacial phenomena in joining of ceramics by active metal brazing alloy, Eng. Fract. Mech., 1991, 40 (4-5): 941-949.

[34] C. Peytour, F. Barbier, A. Revcolevschi, Characterization of ceramic/TA6V titanium alloy brazed joints, J. Mater. Res., 1990, 5 (1): 127-135.

[35] H.Hao, Z. Jin, X. Wang, Influence of brazing conditions on joint strength in

Al2O3/Al2O3 bonding, J.Mater. Sci., 1994, 29: 5041-5046.

[36] P. Martineau, R. Pailler, M. Lahave et al. SiC filament/titanium matrix composites regarded as model composites. II. Fibre/matrix chemical interactions at high temperatures, J. Mater. Sci. 1984, 19, 2749-2770.

[37] T. Yamazaki, A. Suzumura, Role of the reaction product in the solidification of Ag-Cu-Ti filler for brazing diamond, J. Mater. Sci., 1998, 33: 1379-1384.

[38] P.M. Scott, M.N. Nicholas, B. Dewar, Wetting and bonding of diamonds by copper-base binary alloys, J. Mater. Sci., 1975, 10: 1833-1840.

[39] D. Evens, M. Nicholas, P.M. Sott, Wetting and bonding of diamonds by copper-tin-titanium alloys, Ind. Dia. Rev., 1977, 37: 306-309.

[40] A. Suzumura, T. Yamazaki, K, Takahashi et al. Solidification phenomena and bonding strength at the interface of diamond and active-metal-brazing-filler, J. Jpn. Welding Soc., 1994, 12: 509-514.

[41] A.K. Chattopadhyay, L. Chollet, H.E, Hintermann, On performance of brazed bonded monolayer diamond grinding wheel, CIRP Annals, 1991, 40: 347-350.

[42] R.E. Loehman, A.P. Tomsia, Wetting and joining of mullite ceramics by active-metal braze alloys, J. Am. Ceram. Soc., 1994, 77: 271-274.

[43] H.Q. Hao, Z.H. Jin, X.T. Wang, Influence of brazing conditions on joint strength in Al2O3/Al2O3 bonding, J. Mater. Sci., 1994, 29: 5041-5046.

[44] M. Paulasto, J.K. Kivilahti, Formation of interfacial microstructure in brazing of Si3N4 with Ti-activated Ag-Cu filler alloys, Scripta Metall. Mater., 1995, 32: 1209-1995.

[45] C. Tsai, J.C. Nelson, W.W. Gerberich, et al., Studies on the interfaces and adhesion mechanisms in reinforced diamond composite coatings, Thin Solid Films, 1994, 237: 181-186.

[46] H.K. Lee, S.H. Hwang, J.Y. Lee, Effects of the relative contents of silver and copper on the interfacial reactions and bond strength in the active brazing of SiC, J. Mater. Sci., 1993, 28: 1765-1774.

[47] Y.Z. Hsieh, J.F. Chen, S.T. Lin, Pressureless sintering of metal-bonded diamond particle composite blocks, J. Mater. Sci., 2000, 35: 5383-5387.

[48] R.E. Hans, E.K. Ulrich, A.K. Fazal etal. The Role of Binder Content on Microstructure and Properities of a Cu-Base Active Brazing Filler Metal for Diamond and cBN, Advanced Enineering Materials, 2005, v7, n5, 375-380.

[49] W. Li, C. Liang, S. Lin, Interfacial segregation of Ti in the brazing of diamond grits onto a steel Substrate Using a Cu-Sn-Ti Brazing Alloy, Metal. Mater. Trans., 2002, 33A (7): 2163-2172.

[50] B.J. Lee, N.M. Hwang, H.M. Lee, prediction of interface reaction products between Cu and various solder alloys by thermodynamic calculation, Acta mater., 1997, 45(5), 1867-1874.

[51] MASSALSKI T B. Binary Alloy Phase Diagrams[M], OH, USA: ASM International, 2001: 3405.

[52] SHIM J, OH C S, LEE B J, et al. Thermodynamic assessment of the Cu-Sn system[J]. Z. Metallkd, 1996, 87(3): 205-212.

[53] HARI KUMAR K C, ANSARA I, WOLLANTS P, et al. Thermodynamic optimization of the Cu-Ti system[J]. Z. Metallkd,1996, 87(8)1996: 666-672.

[54] E.D. Kizikov, I.A. Lavrinenko, Investigation of Cu-Sn-Ti alloys used for bonding diamond abrasive tools, Met. Sci. Heat Treat., 1975, 17: 61-65.

[55] M. Naka, J. C. Schuster, L. Nakade et al. Determination of the liquidus of the ternary system Cu-Sn-Ti, J. Phase Equil., 22 (2001), 352.

[56] S. Hamar-Thibault, C. Allibert, W. Tillman, EPMA (Ed.), Int Workshop on

Diamond Tools Proc., Turin, 1999, 57.

[57] J.C. Schuster, M. Naka, T. Schibayanagi, Crystal structure of CuSn3Ti5 and related phases, J. Alloys Compds., 305 (2000), L1-L3

[58] S. Hamar-Thibault, C.H. Allibert, New phases in the ternary Cu-Ti-Sn system J. Alloys Compds., 317-318 (2001), 363-366.

[59] W. Heine, U. Zwicker, Naturwiss., 49 (1962), 391.

[60] F. Weitzer, L. Perring, T. Shibayanagi, Naka etc., Determination of the crystal structure of CuSnTi by full profile Rietveld analysis， Powder Diffr., 15 (2000), 91-93.

[61] W. Bader, Dissolution of Au, Ag, Pd, Pt, Cu, and Ni in a molten tin-lead solder, Welding J., 1969, 48 (12): 551-557.

[62] C. Kuper, W. Peng, A. Pisch, F. Goesmann, R. Schmid-Fetzer, Phase formation and reaction kinetics in the system Ti-Sn, Z. Metallkd., 1998, 89 (12): 855-862.

List of Publication

1) 李大建，Cu-Sn-Ti 体系边际二元系界面反应的研究，粉末冶金材料科学与工程， 已接收
2) Dajian Li, Huashan Liu, Libin Liu, Yuan Yuan, Weiping gong, Phase Relations in the Cu-Sn-Ti Ternary System at 823K determined by Diffusion Triple Technique, submitted to Journal of alloys and compounds.
3) Yuan Yuan, Libin Liu, Dajian Li, Zhanpeng Jin, Interfacial Reaction of Sn-Zn/Ni Diffusion Couples, submitted to Acta Metallurgic Sinica.
4) Yuan Yuan, Libin Liu, Dajian Li, Zhanpeng Jin,Interfacial Reaction of Sn-Zn/Ni Diffusion Couples at 873K, submitted.

Acknowledgements

My first thanks go to my supervisor, Professor Jin for his many instructions and concern of my study and life. This thesis could not being accomplished without his help and suggestions.

I express words of gratitude to Professor Huashan Liu, Libin Liu, Yong Du and Feng Zhen, who offer me much guidance.

In addition, I will thank my classmates, Yuan Yuan, who helps me make experiment and analyze the experiment data.

I am grateful to National Natural Science Foundation of China (Grant No. 50371104) and Natural Science Foundation of Guangdong Province (No. 33354) for financial support.